Office de la Propriété Intellectuelle du Canada
Un organisme d'Industrie Canada

Canadian Intellectual Property Office
An agency of Industry Canada

CA 2554302 C 2013/03/26

(11)(21) 2 554 302

(12) BREVET CANADIEN
CANADIAN PATENT

(13) C

(86) Date de dépôt PCT/PCT Filing Date: 2005/01/26
(87) Date publication PCT/PCT Publication Date: 2005/08/25
(45) Date de délivrance/Issue Date: 2013/03/26
(85) Entrée phase nationale/National Entry: 2006/07/25
(86) N° demande PCT/PCT Application No.: US 2005/002385
(87) N° publication PCT/PCT Publication No.: 2005/076815
(30) Priorité/Priority: 2004/01/26 (US60/539,133)

(51) Cl.Int./Int.Cl. *C07D 471/04* (2006.01), *C07D 221/18* (2006.01), *H01L 29/12* (2006.01), *H01L 51/30* (2006.01)

(72) Inventeurs/Inventors:
MARKS, TOBIN J., US;
WASIELEWSKI, MICHAEL R., US;
FACCHETTI, ANTONIO, US;
AHRENS, MICHAEL J., US;
JONES, BROOKS A., US;
YOON, MYUNG-HAN, US

(73) Propriétaire/Owner:
NORTHWESTERN UNIVERSITY, US

(74) Agent: FINLAYSON & SINGLEHURST

(54) Titre : SEMI-CONDUCTEURS DE TYPE PERYLENE N ET DISPOSITIFS ASSOCIES
(54) Title: PERYLENE N-TYPE SEMICONDUCTORS AND RELATED DEVICES

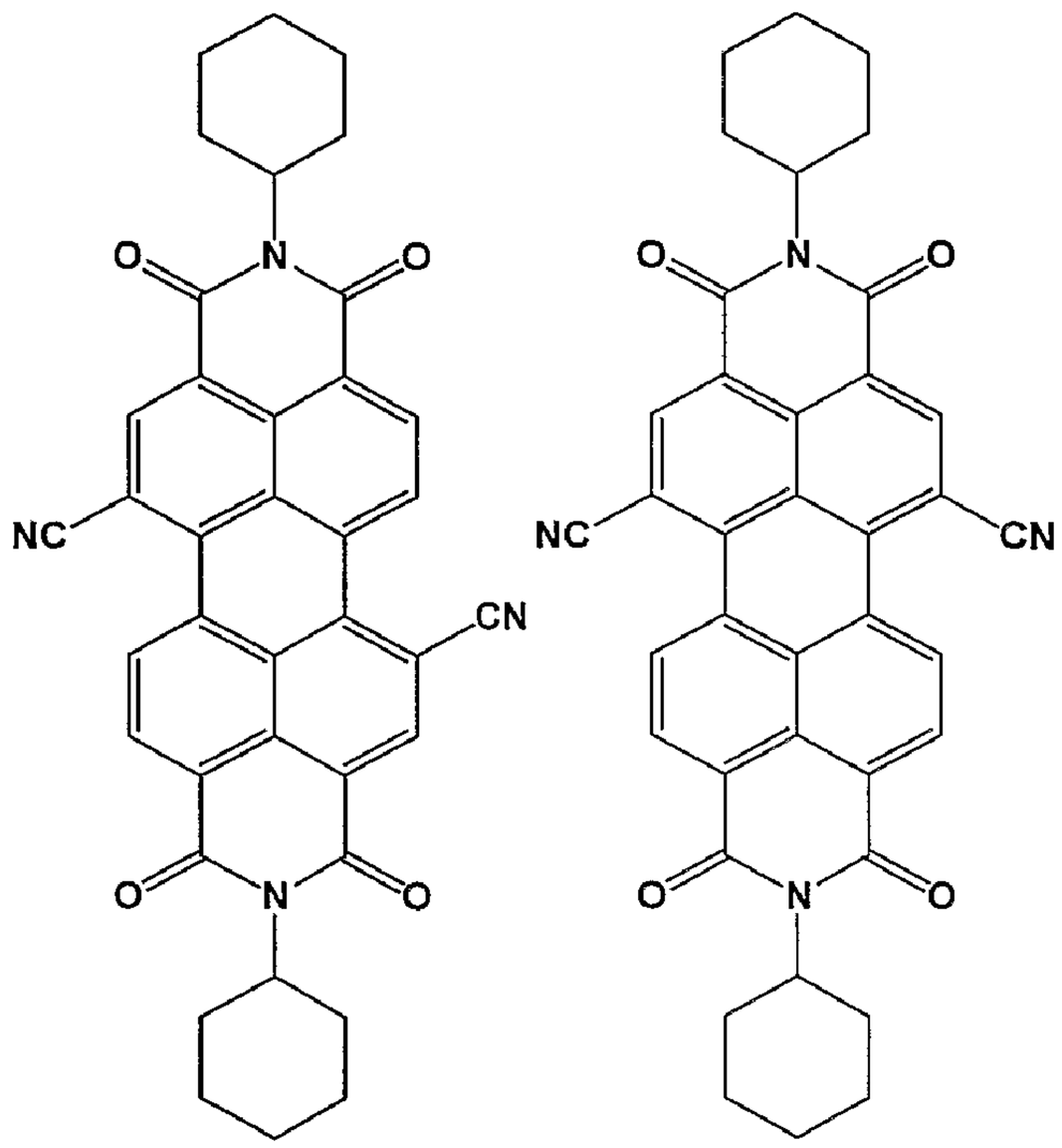

tCN_2PDI

cCN_2PDI

(57) Abrégé/Abstract:
Mono- and diimide perylene and naphthalene compounds, N- and core substituted with electron-withdrawing groups, for use in the fabrication of various device structures.

(12) INTERNATIONAL APPLICATION PUBLISHED UNDER THE PATENT COOPERATION TREATY (PCT)

(19) World Intellectual Property Organization
International Bureau

(43) International Publication Date
25 August 2005 (25.08.2005)

PCT

(10) International Publication Number
WO 2005/076815 A2

(51) International Patent Classification: Not classified

(21) International Application Number:
PCT/US2005/002385

(22) International Filing Date: 26 January 2005 (26.01.2005)

(25) Filing Language: English

(26) Publication Language: English

(30) Priority Data:
60/539,133 26 January 2004 (26.01.2004) US

(71) Applicant *(for all designated States except US)*: **NORTHWESTERN UNIVERSITY** [US/US]; 633 Clark Street, Evanston, IL 60208 (US).

(72) Inventors; and

(75) Inventors/Applicants *(for US only)*: **MARKS, Tobin, J.** [US/US]; 2300 Central Park Avenue, Evanston, IL 60201 (US). **WASIELEWSKI, Michael, R.** [US/US]; 2338 Iroquois Drive, Glenview, IL 60026-1034 (US). **FACCHETTI, Antonio** [IT/US]; 5412 North Glennwood, Chicago, IL 60640 (US). **AHRENS, Michael, J.** [US/US]; 907 Washington Street, Apt G-5, Evanston, IL 60202 (US). **JONES, Brooks, A.** [US/US]; 1024 Foster Street, Apt 2, Evanston, IL 60201 (US). **YOON, Myung-Han** [KR/US]; 522 Greenwood, #GW, Evanston, IL 60201 (US).

(74) Agents: **DEKRUIF, Rodney, D.** et al.; Reinhart Boerner Van Deuren s.c., Attn: Linda Gabriel-Kasulke, Docket Clerk, 1000 North Water Street, Suite 2100, Milwaukee, WI 53202 (US).

(81) Designated States *(unless otherwise indicated, for every kind of national protection available)*: AE, AG, AL, AM, AT, AU, AZ, BA, BB, BG, BR, BW, BY, BZ, CA, CH, CN, CO, CR, CU, CZ, DE, DK, DM, DZ, EC, EE, EG, ES, FI, GB, GD, GE, GH, GM, HR, HU, ID, IL, IN, IS, JP, KE, KG, KP, KR, KZ, LC, LK, LR, LS, LT, LU, LV, MA, MD, MG, MK, MN, MW, MX, MZ, NA, NI, NO, NZ, OM, PG, PH, PL, PT, RO, RU, SC, SD, SE, SG, SK, SL, SY, TJ, TM, TN, TR, TT, TZ, UA, UG, US, UZ, VC, VN, YU, ZA, ZM, ZW.

(84) Designated States *(unless otherwise indicated, for every kind of regional protection available)*: ARIPO (BW, GH, GM, KE, LS, MW, MZ, NA, SD, SL, SZ, TZ, UG, ZM, ZW), Eurasian (AM, AZ, BY, KG, KZ, MD, RU, TJ, TM), European (AT, BE, BG, CH, CY, CZ, DE, DK, EE, ES, FI,

[Continued on next page]

(54) Title: PERYLENE n-TYPE SEMICONDUCTORS AND RELATED DEVICES

(57) Abstract: Mono- and diimide perylene and naphthalene compounds, N- and core substituted with electron-withdrawing groups, for use in the fabrication of various device structures.

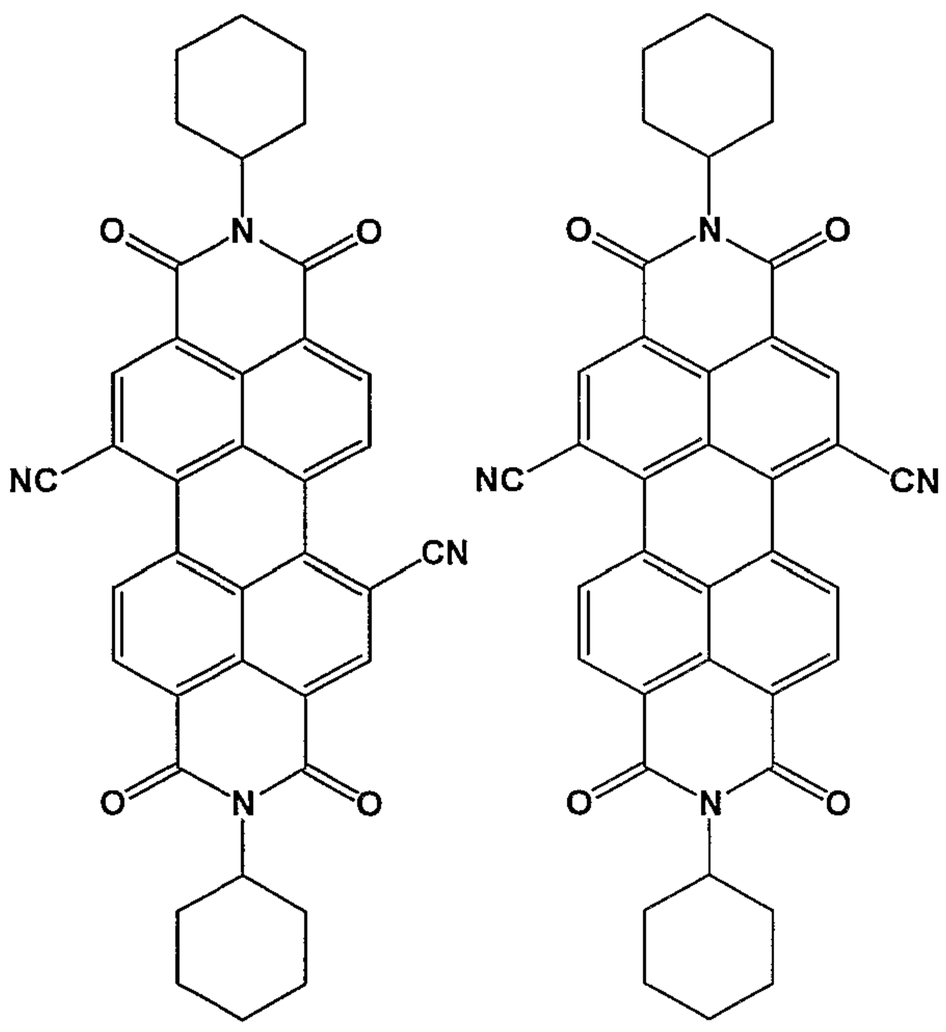

tCN_2PDI *c*CN_2PDI

WO 2005/076815 A2

WO 2005/076815 A2

FR, GB, GR, HU, IE, IS, IT, LT, LU, MC, NL, PL, PT, RO, SE, SI, SK, TR), OAPI (BF, BJ, CF, CG, CI, CM, GA, GN, GQ, GW, ML, MR, NE, SN, TD, TG).

Published:

— *without international search report and to be republished upon receipt of that report*

For two-letter codes and other abbreviations, refer to the "Guidance Notes on Codes and Abbreviations" appearing at the beginning of each regular issue of the PCT Gazette.

PERYLENE n-TYPE SEMICONDUCTORS AND RELATED DEVICES

The United States Government has certain rights to this invention pursuant to Grant Nos. N00014-02-1-0909 (0650-300-F445) and N00014-02-1-0381 from the Office of Naval Research, DARPA Grant No. MDA972-03-1-0023, and Grant No. DMR-0076097 (MRC) from the National Science Foundation, all to Northwestern University.

Background of the Invention.

Organic semiconductors based on molecular and polymeric materials have become a major part of the electronics industry in the last 25 years as a complement to the shortcomings of inorganic semiconductors. Most notably, organic semiconductors offer, with respect to current inorganic-based technology, greater ease in substrate compatibility, device processability, flexibility, large area coverage, and reduced cost; as well as facile tuning of the frontier molecular orbital energies by molecular design. A key device used in the electronic industry is the field-effect transistor (FET) based on inorganic electrodes, insulators, and semiconductors. FETs based on organic semiconductors (OFET) may find niche applications in low-performance memory elements as well as integrated optoelectronic devices, such as pixel drive and switching elements in active-matrix organic light-emitting diode (LED) displays.

The thin-film transistor (TFT), in which a thin film of the organic semiconductor is deposited on top of a dielectric with an underlying gate (G) electrode, is the simplest and most common semiconductor device configuration. Charge-injecting drain–source (D-S) electrodes providing the contacts are defined either on top of the organic film (top-configuration) or on the surface of the FET substrate prior to the deposition of the semiconductor (bottom-configuration). The current between S and D electrodes is low when

no voltage is applied between G and D electrodes, and the device is in the so called 'off' state. When a voltage is applied to the gate, charges can be induced into the semiconductor at the interface with the dielectric layer. As a result, the D–S current increases due to the increased number of charge carriers, and this is called the 'on' state of a transistor. The key parameters in characterizing a FET are the field-effect mobility (μ) which quantifies the average charge carrier drift velocity per unit electric field and the on/off ratio (I_{on}:I_{off}) defined as the D–S current ratio between the 'on' and 'off' states. For a high performance OFET, the field-effect mobility and on/off ratio should both be as high as possible.

Most of the OFETs operate in p-type accumulation mode, meaning that the semiconductor acts as a hole-transporting material. However, for the full development of the field of organic semiconductors, high-performing electron-transporting (n-type) materials are needed as well. For most practical applications, the mobility of the field-induced charges should, optimally, be > 0.1–1 cm^2/Vs. To achieve high performance, the organic semiconductors should also meet or approach certain criteria relating to both the injection and current-carrying phenomena, in particular: (i) HOMO/LUMO energies of individual molecules (perturbed by their placement in a crystalline solid) at levels where holes/electrons may be added at accessible applied voltages, (ii) a crystal structure of the material with sufficient overlap of the frontier orbitals (π stacking and edge-to-face contacts) for charge migration among neighboring molecules, (iii) a compound with minimal impurities as charge carrier traps, (iv) molecules (in particular the conjugated core axes) preferentially oriented with their long axes close to the FET substrate normal, as efficient charge transport occurs along the direction of intermolecular π-π stacking, and (v) uniform coverage of the crystalline semiconductor domains between source and drain contacts, preferably with a film having preferably with a film exhibiting a single crystal-like morphology.

Among n-type organic semiconductors used in OFETs, the class of arene core diimides is one of the most investigated. The first report on a

diimide-based FET was on a series of naphthalene tetracarboxylic diimides, followed by reports of perylene tetracarboxylic diimides. Over the years, chemical modification and tailoring of the imide position has resulted in the production and testing of a library of diimide-based materials. However, such compounds have been found generally to be unstable in air and have solubility characteristics less than satisfactory for efficient device fabrication.

Summary of the Invention.

In light of the foregoing, it is an aspect of the present invention to provide n-type semiconductor compounds and/or devices and related methods for their use, thereby overcoming various deficiencies and shortcomings of the prior art, including those outlined above. It will be understood by those skilled in the art that one or more aspects of this invention can meet certain objectives, while one or more other aspects can meet certain other objectives. Each objective may not apply or apply equally, in all its respects, to every aspect of this invention. As such, the following objects can be viewed in the alternative with respect to any one aspect of this invention.

It is an aspect of this invention to provide one or more of the present polycyclic aromatic mono- and/or diimide compounds core-substituted with one or more electron-withdrawing moieties or groups, and/or the radical anions electrochemically generated therefrom.

It is another aspect of the invention, in conjunction with the preceding, to provide such compounds with a range of available electron withdrawing N-substituted moieties, groups and/or substituents.

It is another aspect of this invention to incorporate any one or more of the present compounds into a range of device structures including but not limited to organic light-emitting diodes, field-effect transistors, and photovoltaic devices.

It is another aspect of the present invention to use compounds of the type described herein to enhance oxidative stability and/or lower reduction potential(s) of such compounds, as compared to un-substituted polycyclic compounds of the prior art.

Other aspects, features, benefits and advantages of the present invention will be apparent from this summary and descriptions of various embodiments, and will be readily apparent to those skilled in the art having knowledge of n-type semiconductor materials, related device structures, and use thereof. Such objects, features, benefits and advantages will be apparent from the above as taken into conjunction with the accompanying examples, data, figures and all reasonable inferences to be drawn therefrom, alone or with consideration of the references incorporated herein.

This invention relates to mono-and diimide perylene and naphthalene compounds functionalized at core and imide positions with varying moieties for improved solubility and radical anion stability, while maintaining strong π–π interactions. The choice of moiety or functional group can vary as described herein but can take into consideration three factors: 1) electron-withdrawing capability, 2) capability of attachment to the π-conjugated core, and/or 3) potential for increased solubility of the compound for solution processing. Such compounds and related methods can be employed to enhance associated device (e.g., OFET) performance.

As described below, electronegative or electron-withdrawing functionalities, such as cyano substituents and fluorinated moieties, when substituted (e.g., N- or core substituted) on highly conjugated naphthalene or perylene structures are shown to improve electron injection—presumably, but without limitation, by facilitating formation of charge carriers in the form of radical anions. To illustrate such effects, a representative series of cyano-substituted perylene imides—with low reduction potentials, high solubility, and interesting optical characteristics—was synthesized. In particular, such core functionalized perylene diimide derivatives demonstrate large chemical/thermal stability and strong π-π intermolecular interactions. Accordingly, these compounds and others of the sort described herein can be used in the fabrication of OFETs and related device structures.

Without limitation as to any one device structure or end-use application, the present invention can relate to n-type semiconductor compounds of a formula selected from

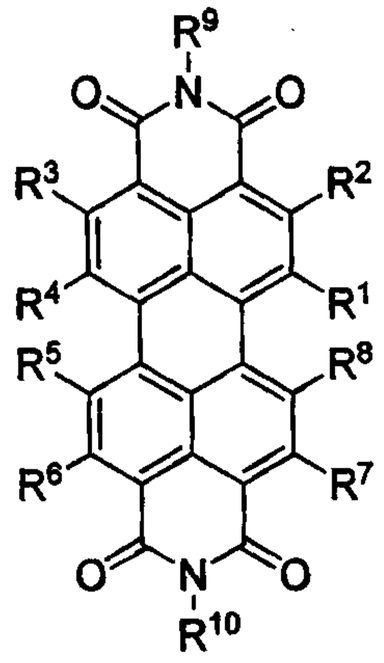

and

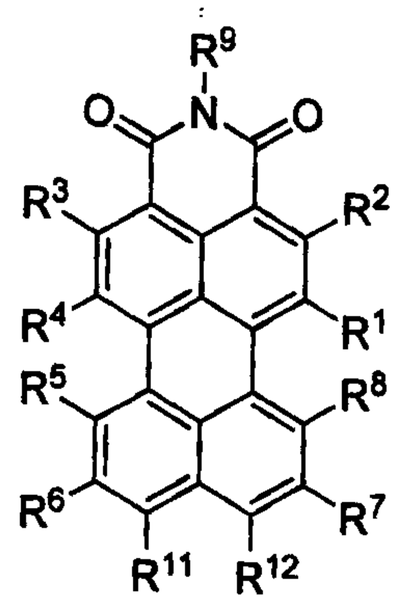

wherein each of R^1-R^8, R^{11}, and R^{12} can be independently selected from H, an electron-withdrawing substituent and a moiety comprising such a substituent. Electron-withdrawing substituents include but are not limited to nitro, cyano, quarteranary amino, sulfo, carbonyl, substituted carbonyl and carboxy substituents. Associated moieties can be but are not limited to alkyl, substituted alkyl, cycloalkyl, substituted cycloalkyl, aryl, substituted aryl, polycyclic aryl and substituted polycyclic aryl moieties. Without limitation, such moieties and associated electron-withdrawing substituents can be selected from C_nF_{2n+1}, $C_nH_2F_{2n-1}$ and C(O)R (e.g., R=H, alkyl, C_nF_{2n+1} or $C_nH_2F_{2n-1}$) groups—as would be understood by those skilled in the art and made aware of this invention. At least one of R^1-R^8, R^{11}, and R^{12} is selected from one of such substituents and/or associated moieties. R^9 and R^{10} are independently selected from H, alkyl, substituted alkyl, cycloalkyl, substituted cycloalkyl, aryl, substituted aryl, polycyclic aryl and substituted polycyclic aryl moieties. Any such moiety can comprise one or more of the aforementioned electron-withdrawing substituents. For example, without limitation, certain substituted alkyl moieties can include C_nH_{2n+1}, C_nF_{2n+1}, $C_nH_2F_{2n-1}$ and the like. Further, one or more methylene (-CH_2-) or methene (-CH=) components of any such

alkyl or aryl moiety can be substituted with a heteroatom (e.g., O or N) to provide the corresponding substituted moiety (e.g., ether, amine, polyether, polyamine and corresponding heteroaromatic moieties).

In certain other embodiments, at least one of R^1, R^4, R^5, R^8, R^{11}, and R^{12} can be either an electron-withdrawing substituent or a moiety comprising such a substituent. In certain other embodiments, such electron-withdrawing substituents can be selected from fluorine and substituents having a Hammett σ^+ value ≥ 0.3. Without limitation, at least one of R^1, R^4, R^5, R^8, R^{11}, and R^{12} can be a cyano substituent. In certain other embodiments, as discussed more fully below, such cyanated compounds can be di- or tetra-substituted, as shown in the following representative structures.

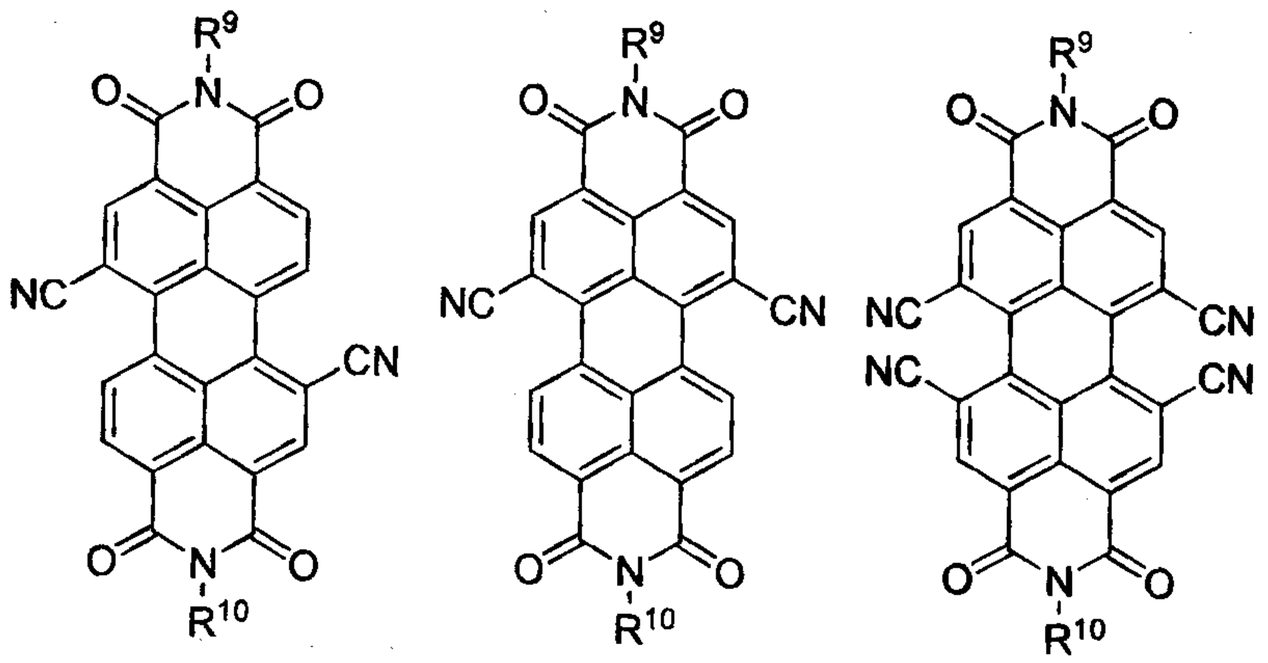

Regardless of core substitution, in certain embodiments, at least one of R^9 and R^{10} can be selected, optionally, fluoro-substituted, regardless of any particular pattern or degree or core substitution.

Likewise, without regard to any particular end-use application, this invention can be directed to composites of the type incorporated into a range of device structures. Such a composite can comprise a suitable substrate; and a semiconductor component, with or without the presence of any additional functional layer, film or component therebetween. Such a semiconductor component can comprise a compound of a formula selected from

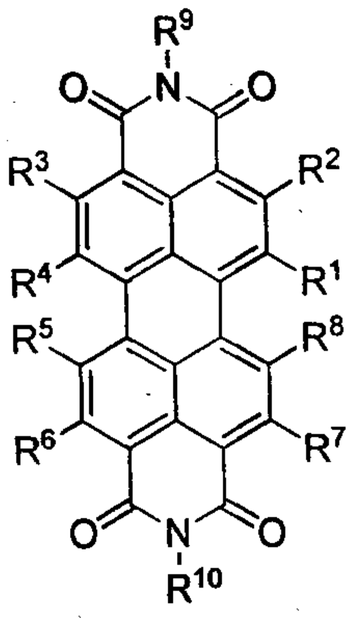

and

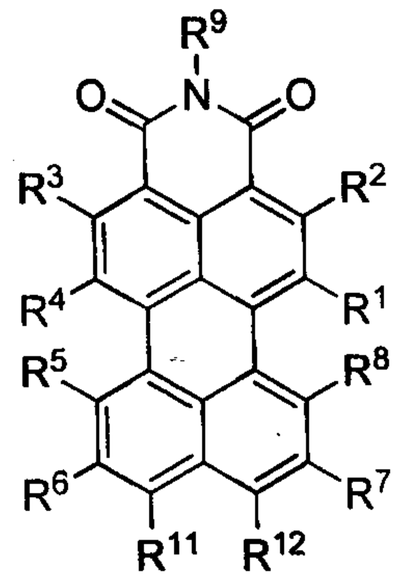

such compounds N- and core-substituted, as described above. In certain embodiments, such a composite can be incorporated into an OFET or another device structure. Regardless, core substitution can be used to enhance oxidative stability and/or to lower the reduction potential(s) of such a compound, as compared to unsubstituted perylene compounds of the prior art, and improve device performance.

In part, the present invention can also be directed to n-type semiconductor compounds of a formula selected from

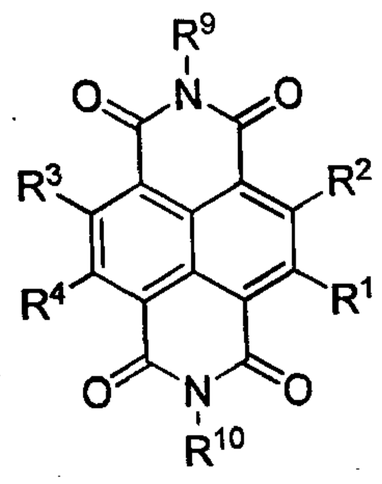

and

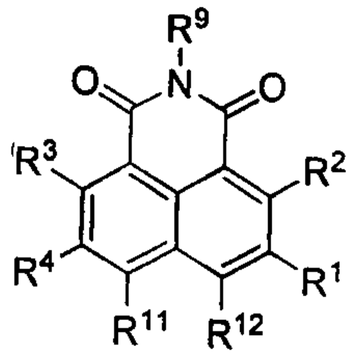

wherein R^1-R^4, R^{11}, and R^{12} are independently selected from H and a cyano substituent, such that the compound is dicyano-substituted. R^9 and R^{10} can be independently selected from H and moieties of the type described above in conjunction with various representative perylene compounds, such moieties as can be further substituted with one or more electron-withdrawing substituents

of the sort described herein. Such compounds can be used as illustrated below for enhanced oxidative stability and/or to lower the reduction potential of such compounds as compared to unsubstituted naphthalene.

With respect to compounds, composites and/or methods of this invention, the compounds can suitably comprise, consist of, or consist essentially of any one or more of the aforementioned substituents and/or moieties. Each such compound or moiety/substituent thereof is compositionally distinguishable, characteristically contrasted and can be practiced in conjunction with the present invention separate and apart from one another. Accordingly, it should also be understood that the inventive compounds, composites and/or methods, as illustrated herein, can be practiced or utilized in the absence of any one particular compound, moiety and/or substituent—such compound, moiety and/or substituent which may or may not be specifically disclosed or referenced, the absence of which may not be specifically disclosed or referenced.

Brief Description of the Drawings.

Figure 1. Electronic absorption and fluorescence (inset) spectra of the indicated compounds in toluence. Fluorescence spectra were obtained following excitation at 480-490 nm.

Figure 2. Electronic absorption spectra of CNPMI and CN_3PMI in butyronitrile containing 0.1 M Bu_4NPF_6 and 0.1 M Bu_4NC1O_4, respectively, following controlled potential electrolysis at -0.9 and -0.3 V vs SCE, respectively.

Figure 3. Electronic absorption spectra of CN_2PDI^- and CN_2PDI^{2-} in DMF containing 0.1 M Bu_4NC1O_4 following controlled potential electrolysis at -0.1 V vs SCE and at -0.6 V vs SCE, respectively.

Figure 4. Selected non-limiting dicyano compounds, *t*CN_2PDI and *c*CN_2PDI.

Figure 5. UV-vis absorption and photoluminescence (PL) spectra of *t*CN_2PDI and *c*CN_2PDI.

Figure 6. X-ray diffraction data on a CN_2 PDI thin-film grown at room temperature and at a 90°C substrate temperature.

Figure 7. AFM analysis of CN_2PDI thin films grown at substrate temperatures of 25 °C and 90°C.

Figure 8. SEM analysis of a CN_2PDI thin film grown at 90°C substrate temperature.

Figure 9. FET current-voltage characteristics of CN_2PDI under different positive gate-source biases in vacuum, N_2, in air after 12 hours, in air after 5 days.

Figure 10. Schematic illustration of a spectroelectrochemical cell of the type used herein to characterize compounds of this invention.

Figure 11. CN_2PDI (10^{-5}M) in dry DMF, ambient oxygen (solid line). Progressive increase over 15 min. of CN2PDI^{-} spectrum while N_2 is bubbled into the cuvette (all other lines).

Figure 12. Crystal structure of PDI-FCN_2 a) viewed along the unit cell diagonal, showing stacking relationships; fluoropropyl groups deleted for clarity; b) viewed along the *ab* face diagonal, showing the segregation of arene and fluoroalkyl groups. Note the statistical disorder of the cyano substituents.

Figure 13. a) I-V characteristics of PDI-CN_2 exhibiting a mobility of 0.10 $cm^2 V^{-1} s^{-1}$ in ambient atmosphere b) I-V characteristics of a PDI-FCN_2 FET exhibiting a mobility of 0.64 $cm^2 V^{-1} s^{-1}$ in ambient atmosphere.

Figure 14. A graphic representation of the longevity and stability available from an OFET comprising a PDI-FCN2 thin film, showing minimal change in mobilities during cycling.

Figure 15. TGA scan of FCN_2 PDI and CN_2PDI at 2 Torr. The temperature ramp rate is 1.5 °C/ min.

Figure 16. SEM micrographs of 50 nm thick films of a) PDI-FCN_2 deposited on a 1 °C HMDS-treated Si(100) substrate and b) PDI-CN_2 deposited on a 90 °C HMDS-treated Si(100) substrate.

Figure 17. Tapping mode AFM images of a) PDI-FCN_2 deposited on Si(100) at 110 °C and b) PDI-CN_2 deposited on Si(100) at 90 °C.

Figure 18. Thin film Θ-2Θ X-ray diffraction from PDI-FCN_2 and PDI-CN_2 films deposited on Si(100) at 110 °C and 90 °C, respectively. Reflections are assigned for PDI-FCN_2 from the single crystal diffraction data.

Figure 19: I-V Curve for an organic transistor comprising a semiconductor film of PDI-$8CN_2$ deposited at 130 °C.

Detailed Description of Certain Embodiments.

Various features and benefits of this invention can be illustrated through the preparation and characterization of certain non-limiting n-type semiconductor compounds, such as the following mono-cyano (CN) di-cyano (CN_2) and tri-cyano (CN_3) mono-imide (MI) and diimide (DI) perylene compounds. Such compounds and their electrochemically-generated radical anions are shown to serve as stable, photochemical oxidants in a range of novel photonic and electronic films, materials and related device structures.

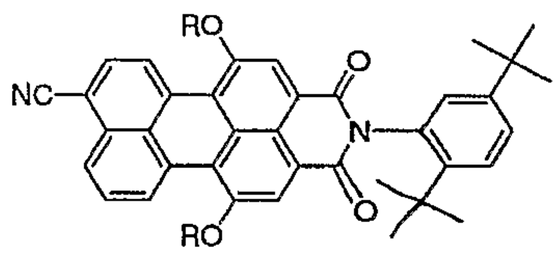

CNPMI R = 3,5-di-*tert*-butylphenyl

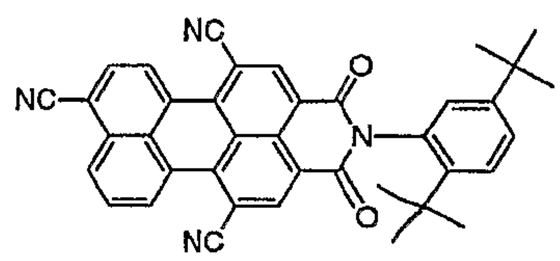

CN_3PMI

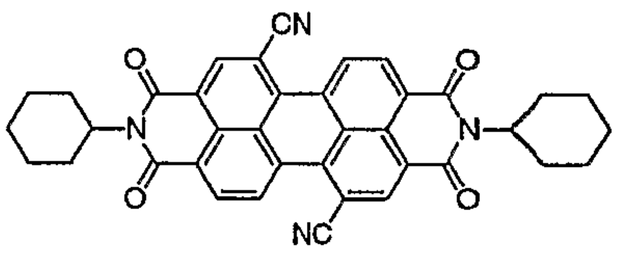

CN_2PDI

The immediate precursors to such cyanoperylenes are the corresponding bromo derivatives: *N,N*-dicyclohexyl-1,7-dibromoperylene-3,4:9,10-bis(dicarboximide), *N*-(2,5-*tert*-butylphenyl)-9-bromoperylene-3,4-dicarboximide, and *N*-(2,5-*tert*-butylphenyl)-1,6,9-tribromoperylene-3,4-dicarboximide, which are readily synthesized in high yields by direct bromination of the parent hydrocarbons. Classical cyanation procedures using

CuCN in refluxing DMF failed to produce the desired cyano compounds. In all three cases this procedure resulted in significant yields of debrominated products. Recently, $Zn(CN)_2$ or CuCN in the presence of a Pd(0) catalyst has been used to

Table 1. Photophysical and Electrochemical Properties

compd	λ_{abs} (nm) ϵ (M^{-1} cm^{-1})	λ_{em} (nm)	E_S (eV)	φ_F	$E^{-}_{1/2}$ (V)	$E^{2-}_{1/2}$ (V)
CN_2PDI	530 47000	545	2.30	1.0	−0.07[a]	−0.40[a]
CNPMI	515 61000	541	2.35	0.91	−0.73[b]	−1.14[b]
CN_3PMI	522 60000	554	2.30	0.83	−0.19[a]	−0.72[a]

[a] Butyronitrile + 0.1 M Bu_4NClO_4. [b] Butyronitrile + 0.1 M Bu_4NPF_6. Electrochemical potentials vs SCE absorption spectroscopy, even when they are in the presence of other perylene derivatives.

convert bromoarenes into cyanoarenes in excellent yields. The $Zn(CN)_2$ method was used to quantitatively convert all three bromoperylene derivatives to the corresponding cyano compounds, as described in the following examples.

The ground-state absorption and emission spectra of the neutral molecules in toluene are shown in Figure 1. The intense absorbance maxima for each of these chromophores are near 500 nm and are only slightly shifted in wavelength relative to those of unsubstituted PMI (512 nm) and PDI (526 nm). In addition to the usual vibronic progression present in each of these rigid aromatic molecules, the spectrum of CNPMI shows an additional band at 420 nm, which is typical of 1,6-bisphenoxylated PMI derivatives. The 420-nm band partially obscures the second vibronic band of CNPMI at 450 nm. The cyanated derivatives all fluoresce with quantum yields $\varphi_F > 0.8$, determined relative to rhodamine 640 (Table 1). The absorption and emission features of these molecules are not solvatochromic, which coupled with the high fluorescence quantum yields suggest that their lowest excited singlet states possess little or no charge-transfer character. The energies of the lowest excited singlet states, E_S, were estimated by averaging the energies of their absorption and emission maxima, λ_{abs} and λ_{kem}, respectively.

Cyclic voltammetry on the cyanated derivatives shows that the one-electron reduction potentials ($E^{-}_{1/2}$ and $E^{2-}_{1/2}$) of each molecule are more positive than those of the unsubstituted analogues (PMI: $E^{-}_{1/2}$ = -0.96, $E^{2-}_{1/2}$ = -1.55 V; PDI: $E^{-}_{1/2}$ = -0.43 V, $E^{2-}_{1/2}$ = -0.70 V, all vs SCE)[13] (Table 1). CN_2PDI and CN_3PMI show exceptionally large positive shifts in redox potential. Spectroelectrochemical measurements yield the electronic absorption spectra of the radical anions of CNPMI, CN_3-PMI, and CN_2PDI and the dianion of CN_2PDI.

The electronic absorption spectra of $CNPMI^{\cdot-}$ and $CN_3PMI^{\cdot-}$ in butyronitrile (Figure 2) show that the absorption characteristics of the neutral molecules are replaced by new bands in the visible spectrum upon reversible electrochemical reduction of the chromophore to its radical anion. For example, the spectrum of $CNPMI^{\cdot-}$ is characterized by an intense absorption band at 644 nm, with minor bands at 480 and 735 nm. The spectrum of $CN_3PMI^{\cdot-}$ is similar to that of $CNPMI^{\cdot-}$ with an intense band at 595 nm and weaker bands at 458 and 680 nm. These bands can be compared to the corresponding intense absorption of $PMI^{\cdot-}$ at 588 nm.

Figure 3 shows the electronic absorption spectra of $CN_2PDI^{\cdot-}$ and CN_2PDI^{2-} obtained by controlled potential electrolysis of CN_2PDI, first at -0.1 V vs SCE and then at -0.6 V vs SCE. At the more negative potential, $CN_2PDI^{\cdot-}$ is cleanly and reversibly converted to CN_2PDI^{2-} as noted by the isosbestic point at 650 nm. The intense absorption band of $CN_2PDI^{\cdot-}$ at 691 nm is blue-shifted relative to that of $PDI^{\cdot-}$ at 712 nm, while the corresponding absorption band of CN_2PDI^{2-} at 628 nm is red-shifted relative to that of PDI^{2-} at 570 nm. The relatively sharp band-width of these absorption features should make it possible to readily identify the presence of these radical anions and dianions as intermediates in electron-transfer reactions using transient absorption spectroscopy, even when they are in the presence of other perylene derivatives.

Under the synthetic preparation described, CN_2PDI (or, alternatively, designated PDI-CN_2, below) appears to be an approximately 50/50 mixture of *t*CN_2PDI and *c*CN_2PDI as shown by NMR. (Fig. 4) Figure 5 shows optical

spectra in a THF solution. By combining the electrochemical and optical data, absolute orbital energies can be estimated. LUMO energies can be determined from the first reduction potentials and HOMO energies considering the optical gap. The HOMO level is estimated to be at –7.10 eV and the LUMO level to be at –4.77 eV. These low lying MO energy levels allow for facile electron injection.

To demonstrate the effectiveness of CN_2PDI as a strong oxidant, the spectrum of this compound was monitored in the presence of an oxidizable species. For example, a 10^{-5} M solution of CN_2PDI in dry DMF shows an absorption feature at 691 nm, indicating that about 15% of CN_2PDI is converted to $CN_2PDI^{\cdot-}$ under ambient oxygenated conditions. Bubbling dry N_2 through the solution for 15 min produces a dramatic increase in the intensity of the $CN_2PDI^{\cdot-}$ spectrum, indicating about 60% conversion to the radical anion. Since DMF typically contains a small amount of *N,N*-dimethylamine due to decomposition, it is possible that CN_2PDI oxidizes the amine. The aminium radical cation decomposes rapidly, yielding a proton, which is the counterion for the stable $CN_2PDI^{\cdot-}$. This same effect can be observed in toluene, which is not oxidized by CN_2PDI, by adding a small amount of triethylamine to the toluene solution. While the first reduction potential of CN_2PDI is very similar to the well-known oxidant, chloranil ($E[A/A^{\cdot-}] = 0.02$ V vs SCE), the radical anion and dianion of CN_2PDI, unlike the reduced chloranil species, are excellent chromophores themselves and are not susceptible to decomposition through irreversible protonation reactions. Moreover, both CN_2PDI and CN_3PMI are significantly easier to reduce than C_{60} ($E[A/A^{\cdot-}] = -0.38$ V vs SCE), which is a typical electron acceptor in organic materials.

The film-forming properties of CN_2PDI were examined by X-ray diffraction, AFM, and SEM. (See, Figs. 6-8.) Depending on chemical nature of the system, highly ordered or amorphous films can be produced as a function of deposition method (evaporation, spin-coating, casing), substrate temperature, and/or substrate pretreatment. For small molecules it is widely accepted that evaporation gives higher quality films; hence, analysis of the

following films. X-ray diffraction reveals a d-spacing within the film of 17.9 Å. Based on a MM geometry optimization calculation, the length of these molecules is 22 Å. The tilt angle to the substrate normal is thus 35.3 °. AFM data shows that films grown on a pretreated 90°C substrate give the smoothest, most contiguous morphology.

A top-contact configuration was used to fabricate field effect transistor devices. The semiconductor mixture was vacuum-deposited on top of HMDS-treated Si/SiO_2 substrates kept at the temperature (T_D) of 25 and 90°C. The electrical measurements were performed under vacuum (~ 10^{-4} Torr), $N_{2(g)}$, and in ambient atmosphere. The FET devices of this invention were fabricated as provided above and further described in U.S. Patent No. 6,608,323, in particular Example 16 and Fig. 8 thereof, the entirety of which may be referred to for further details.

Figure 9 shows typical drain-source current/voltage plots of CN_2PDI operating at different gate bias in three atmospheric conditions. For purposes of comparison with other organic FETs, the mobilities were calculated by standard field effect transistor equations. In traditional metal-insulator-semiconductor FETs (MISFETs) there is typically a linear and saturated regime in the I_{DS} vs V_{DS} curves at different V_G. At large V_{DS} the current saturates and is given by equation (1)

$$(I_{DS})_{sat} = (WC_i / 2L)\ \mu\ (V_G - V_t)^2 \qquad (1)$$

where L and W are the device channel length and width, respectively, C_i is the capacitance of the insulator (1 x 10^{-8} F/cm^2 for 300 nm SiO_2). The mobility (μ) and the threshold voltage (V_t) can be calculated from the slope and intercept, respectively, of the linear section of the plot of V_G versus $(I_{sd})^{1/2}$ (at V_{sd} = -100 V). From these data n-type mobilities approaching 0.1 cm^2/Vs, current on/off ratio of 10^5, and Vt of ~ 14 V were obtained in vacuum and N_2 atmospheres. Upon operation in air, mobilities of 0.05 cm^2/Vs were obtained. Optimization

of film growth and materials purification will doubtless yield far higher mobilities.

The results with PDI-CN_2-derived OFETs (see below) suggested synthesis of another representative PDI derivative with additional electron-withdrawing substituents and greater volatility, e.g., an N-fluoroalkylsubstituted diimide designated PDI-FCN_2.

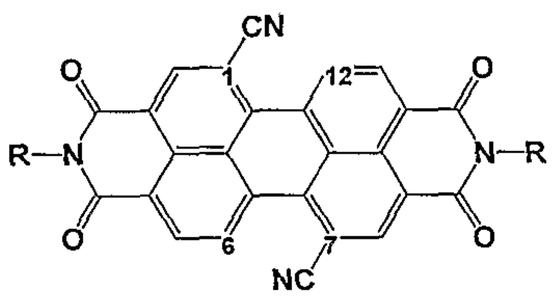

PDI-CN_2 : R = 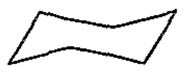

PDI-FCN_2 : R = *n*-$CH_2C_3F_7$

This compound was synthesized using modifications of literature core cyanation and *N*-fluoroalkylation procedures, and was characterized by heteronuclear NMR, mass spectrometry, optical absorption spectroscopy, photoluminescence, cyclic voltammetry, thermogravimetric analysis, and single-crystal x-ray diffraction. The electrochemical and optical data (Table 2) reveal further depression of the LUMO level vs. PDI/PDI-CN_2, while TGA indicates quantitative sublimation.

As mentioned above, for both PDI materials, a 1:1 mixture of isomers (cyanated at the 1,7 or 1,6 positions) is indicated by NMR, however this characteristic is found to be inconsequential for spectroscopic, electronic structural, and solid state charge transport properties (verified by measurements on small quantities of the pure 1,7 isomer). Single crystals of PDI-FCN_2 were grown by sublimation, and the crystal structure (Figure 12) reveals a slightly twisted polycyclic core (torsional angle of ~5°) with slip-stacked face-to-face molecular packing and a minimum interplanar spacing of 3.40 Å. This motif appears to allow considerable intermolecular π-π overlap, resulting in good charge transport properties (see below). The positions of the disordered cyano substituents argues that this structural feature does not greatly affect packing.

Table 2. Electronic and OFET characteristics of perylene diimide derivatives.

Compound	λ_{abs} (nm)[a]	λ_{em} (nm)[a]	$E_{(1)}$ (V)[b]	$E_{(2)}$ (V)[b]	μ ($cm^2 V^{-1} s^{-1}$)	I_{on}/I_{off}
PDI-CN_2	530	547	-0.07	-0.40	0.10	10^5
PDI-FCN_2	530	545	+0.04	-0.31	0.64	10^4

[a] measured in THF ($10^{-5}/10^{-6}$ M)
[b] measured in 0.1 M $TBAPF_6$ solution in THF vs. S.C.E.

For purpose of comparison, top-contact configuration OFETs were fabricated, as described below, with vapor-deposited PDI films (10^{-6} Torr, 0.2 Å/s growth), and mobilities determined in the saturation regime by standard procedures. [a) A. Facchetti, Y. Deng, A. Wang, Y. Koide, H. Sirringhaus, T. J. Marks, R. H. Friend, *Angew. Chem. Int. Ed. Engl.* 2000, *39*, 4547; b) A. Facchetti, M. Mushrush, H. E. Katz, T. J. Marks, *Adv. Mater.* 2003, *15*, 33; c) A. Facchetti, M.-H. Yoon, C. L. Stern, H. E. Katz, T. J. Marks, *Angew. Chem. Int. Ed. Engl.* 2003, *42*, 3900.] The microstructures and mobilities of the vapor-deposited films are found to be sensitive to substrate temperature during growth. Due to the remarkable air-stability of these materials, all data presented here were acquired under ambient atmosphere (Figure 13). PDI-CN_2-based OFETs display mobilities as high as 0.10 $cm^2 V^{-1} s^{-1}$, threshold voltages of ~15 V, and I_{on}/I_{off} (+100 V/ 0 V) ~ 10^5, while PDI-FCN_2 devices exhibit mobilities as high as 0.64 $cm^2 V^{-1} s^{-1}$, threshold voltages between -20 V and -30 V, and I_{on}/I_{off} (+100 V/-60 V) as high as ~10^4. Such mobilities are the highest values reported to date. Devices stored and tested under ambient conditions exhibit negligible degradation in mobility, threshold voltage, or I_{on}/I_{off} over the course of six months.

The microstructure of the vapor-deposited thin films was analyzed by XRD, AFM, and SEM, with XRD revealing *d*-spacings in highest-mobility devices of 17.9 Å and 20.3 Å for PDI-CN_2 and PDI-FCN_2, respectively. From a geometry-optimized, computed molecular length of 22.0 Å for PDI-CN_2 (Hyperchem (TM) 5.02,Hypercube, Inc.,1115 NW 4th Street, Gainesville, FL 32601, USA) and a crystallographically determined length of 22.8 Å for PDI-FCN_2, tilt angles relative to the substrate normal of 55° and 62°, respectively, are estimated. These results suggest favorable molecular orientations for

source-to-drain electrode charge transport. AFM and SEM analysis of film morphology confirms polycrystalline topographies with ribbon-like grains (~ 400-800 nm long, ~100 nm wide). Such large-grained polycrystalline features should promote charge carrier mobility via efficient $\pi-\pi$ intermolecular overlap and minimization of trap sites.

To investigate material versatility for applications, preliminary studies on bottom-contact OFETs and solution-cast films were performed. The bottom-contact devices display air-stable mobilities from 10^{-3} to 10^{-4} cm^2 V^{-1} s^{-1}. PDI-FCN_2 transistors, like many fluorinated organic semiconductors, can be used with alkane thiol treatment of gold electrodes to better match surface energies at the metal/organic interface. Interestingly, PDI-CN_2 devices function without the aid of thiolated electrodes, retaining the ability of PDI to function on unmodified substrates. Top-contact devices fabricated from drip-cast films are also air-stable and exhibit mobilities of 10^{-3} to 10^{-5} cm^2 V^{-1} s^{-1}. In contrast, solution casting of high-quality films of PDI derivatives not having core functionalization is difficult due to low solubility in common solvents.

One of the unique characteristics of such PDI systems is the presence of significant charge carrier densities at $V_G = 0$ V. Thus, OFET threshold voltages for these materials are at $V_G = -20$ V to -30 V, with the absence of charge carriers then defining the 'off' state at – 60 V, and classifying these devices as "always on" transistors. In some cases, the presence of charge carriers below $V_G = 0$ V can be reversed by exposure to an oxidant, and for our devices, I_2 vapor increases the threshold voltage to > -5 V and decreases the I_{SD} at $V_G = 0$ V by up to an order of magnitude.

Of particular note is the air-stability of operation for PDI-FCN_2 and PDI-CN_2-based OFETs. It is thought that ambient stability in n-type organic semiconductors benefits from electron-withdrawing fluorinated substituents, which electronically stabilize the charge carriers as well as promote close packing via fluorocarbon self-segregation. Judging from the present redox potentials, the charge carriers are not initially expected to be thermodynamically stable with respect to $O_2(g)$; however, the close-packed

fluorine functionalities may help provide a kinetic barrier to oxidation. The strategic cyanation of PDI produces air-stable *N*-fluoroalkyl and *N*-alkyl materials, presumably reflecting carrier stabilization in the very low-lying LUMOs.

As shown above, this invention provides solution processable, polycyclic n-type organic semiconductors with high carrier mobility and air-stable OFET operation. Notable properties reflect a combination of electron withdrawing functionality at the core and/or imide positions. In particular, without limitation to any one theory or mode of operation, cyano substitution provides solubility for solution processing and stability of negatively charged polarons by lowering the LUMO to resist ambient oxidation. Likewise, electron-withdrawing *N*-functionalities are believed to aid polaron stability by further lowering the LUMO energies, but may also induce close molecular packing for increased intermolecular π–overlap and more efficient charge transport. With the rich chemistry for PDI functionalization available, various other derivatives—as would be known in the art by those aware of this invention—should prove informative in elucidating structure-function relationships in organic n-type electronics.

Examples of the Invention.

The following non-limiting examples and data illustrate various aspects and features relating to the compounds, devices and/or methods of the present invention, including the use of various mono- and diimide, N- and core-substituted perylene and/or naphthalene compounds as n-type semiconductors and/or in conjunction with field effect transistor devices. Such substituted compounds are available through the synthetic methodologies described herein. While the utility of this invention is illustrated through the use of several such compounds, it will be understood by those skilled in the art that comparable results are obtainable with various other compounds, substituents, and/or substitution patterns, via precursor compounds either commercially available or as described in the literature and substituted as provided herein or using known

reagents and straightforward variations of such synthetic techniques, as would be understood by those skilled in the art made aware of this invention.

General Information for characterization of CN_2PDI, CNPMI and CN_3PMI. ^1H nuclear magnetic resonance spectra were recorded on a Varian 400 MHz NMR spectrometer using TMS as an internal standard. Laser desorption mass spectra were obtained with a Perseptive BioSystems time-of-flight MALDI mass spectrometer using a 2-hydroxy-1-naphthoic acid or dithranol matrix.

Spectroscopy. Absorption measurements were made on a Shimadzu (UV-1601) spectrophotometer using 0.2 cm path length cuvettes. Fluorescence quantum yields were obtained by integrating the fluorescence emission bands from each compound and rhodamine 640 using corrected spectra obtained on a PTI photon-counting spectrofluorimeter with 1 cm path length cuvettes. The absorbance of each sample was < 0.1 at the excitation wavelength.

Electrochemistry. Electrochemical measurements were performed using a CH Instruments Model 660A electrochemical workstation. The solvents were butyronitrile containing 0.1 M tetra-*n*-butylammonium perchlorate or hexafluorophosphate electrolyte. A 1.0 mm diameter platinum disk electrode, platinum wire counter electrode, and Ag/Ag_xO reference electrode were employed. The ferrocene/ferrocinium (Fc/Fc^+, 0.52 vs. SCE) was used as an internal reference for all measurements.

Spectroelectrochemistry. Spectroelectrochemical measurements were performed in the homemade quartz cell illustrated in Figure 10. The cell consists of a 1 mm path length rectangular screw top spectrophotometric cuvette that is screwed into the bottom of a Teflon beaker. Platinum gauze, 100 mesh, woven from 0.07 mm diameter wire was used as a transparent working electrode. The electrode was placed in the 1 mm spectrophotometric cell and connected to the potentiostat (CH Instruments Model 660A) output by a platinum wire. The platinum wire counter and silver wire reference electrodes were placed in the Teflon reservoir, which held a solution of 0.1 M tetra-n-butylammonium perchlorate or hexafluorophosphate in butyronitrile.

The electrochemical workstation controlled the potential of the working electrode, and a Shimadzu 1610A UV-VIS spectrometer obtained the absorption spectra of the redox species. All electrochemical measurements were carried out under a blanket of argon. A series of absorption spectra of the samples were taken until the potential induced spectral evolution was complete, which usually took 7 or 8 minutes.

Example 1

N,N-bis(cyclohexyl)-1,7-dicyano-perylene-3,4:9,10-bis(dicarboximide) (CN_2PDI). *N,N*-bis(cyclohexyl)-1,7-dibromo-perylene-3,4:9,10-bis(dicarboximide) (0.048 g, 0.07 mmol), zinc cyanide (0.065 g, 0.55 mmol), 1,1'-bis(diphenylphosphino)-ferrocene (0.005 g, 0.01 mmol) and tris(dibenzylideneacetone)-dipalladium(0) (0.010 g, 0.01 mmol) were combined in 4 ml p-dioxane and refluxed for 19 hours under a nitrogen atmosphere. The crude product was diluted with chloroform, filtered through Celite, and the solvent removed on a rotary evaporator. The crude product was chromatographed on a silica column using 98 % DCM / 2 % acetone as the eluent to yield 0.041 g product CN_2PDI (theory 0.041 g, quantit). ^{1}H NMR ($CDCl_3$): 9.692 (d, J = 8.1 Hz, 2H), 8.934 (s, 2H), 8.888 (d, J = 8.1 Hz, 2H), 5.025 (m, 2H), 2.533 (m, 4H), 1.931 (m, 4H), 1.755 (m, 6H), 1.504 (m, 4H), 1.329 (m, 2H). M.S.(EI) : Calcd. for $C_{38}H_{28}N_4O_4$: 604.2105, Found: 604.2108.

Example 2

N-(2,5-di-*tert*-butylphenyl)-9-cyano-1,6-bis(3,5-di-*tert*-butylphenoxy)-perylene-3,4-dicarboximide (CNPMI). *N*-(2,5 -di-tert-butylphenyl)-9-bromo-1,6-bis(3,5-di-*tert*-butylphenoxy)-perylene-3,4-dicarboximide (0.100 g, 0.10 mmol), zinc cyanide (0.047 g, 0.40 mmol), 1,1 'bis(diphenylphosphino)-ferrocene (0.009 g, 0.02 mmol) and tris(dibenzylideneacetone)-dipalladium(0) (0.003 g, 0.003 mmol) were combined in 10 ml p-dioxane in a 25 ml round-bottom flask and heated to reflux for 36 hours under a N_2 atmosphere. Upon cooling to room temperature, the crude reaction mixture was diluted with chloroform, washed twice with water, and the solvent removed on a rotary evaporator. The crude product was flash chromatographed on a silica column

using a 65% hexanes/35% chloroform mixture as the eluent to afford 0.094 g product (CNPMI) (theory 0.094 g, quantitative). ^{1}H NMR ($CDCl_3$): 9.525 (d, J = 8.7 Hz, 1H), 9.422 (d, J = 8.2 Hz, 1H), 8.342 (d, J = 7.4 Hz, 1H), 8.281 (s, 2H), 8.021 (d, J = 8.2 Hz, 1H), 7.844 (t, J = 8.1 Hz, 1H), 7.516 (d, J = 8.6 Hz, 1H), 7.394 (d, J = 8.7 Hz, 1H), 7.305 (s, 2H), 7.020 (s, 4H), 6.952 (s, 1H), 1.2-1.4 (s, 72H). M.S.(EI): Calcd. for $C_{65}H_{70}N_2O_4$: 942.5330, Found: 942.5320.

Example 3

N-(2,5-di-*tert*-butylphenyl)-1,6,9-tricyano-perylene-3,4-dicarboximide (CN_3PMI). *N*-(2,5-di-*tert*-butylphenyl)-1,6,9-tribromo-perylene-3,4-dicarboximide (0.082 g, 0.11 mmol), zinc cyanide (0.156 g, 1.33 mmol), 1,1'bis(diphenylphosphino)-ferrocene (0.009 g, 0.02 mmol) and tris(dibenzylideneacetone)-dipalladium(0) (0.004 g, 0.004 mmol) were added to 5 ml p-dioxane and heated to reflux for 16 hours under a N_2 atmosphere. The reaction mixture was diluted with methylene chloride, filtered through Celite, and the solvent removed on a rotary evaporator. The crude product was flash chromatographed on a silica column using methylene chloride as the eluent to give 0.062 g product CN_3PMI (theory 0.064g, 97 %). ^{1}H NMR (CDCl3): 9.603 (d, J = 8.8 Hz, 1H), 9.532 (d, J = 7.3 Hz, 1H), 9.048 (s, 2H), 8.638 (d, J = 7.3 Hz, 1H), 8.248 (d, J = 7.3 Hz, 1H), 8.096 (t, J = 7.3 Hz, 1H), 7.608 (d, J = 8.8 Hz, 1H), 7.495 (d, J = 8.8 Hz, 1H), 6.967 (s, 1H), 1.328 (s, 9H), 1.283 (s, 9H). M.S.(EI): Calcd. for $C_{39}H_{28}N_4O_2$: 584.2207, Found: 584.2199.

Example 4

Oxidation Experiment. A 10^{-5}M solution of CN_2PDI in dry DMF under ambient oxygen conditions was placed in a cuvette and the spectrum was recorded by a Shimadzu 1601 uv-vis spectrophotometer. The solid line in Figure 11 is that spectrum. Dry N_2 was bubbled into the cuvette over a period of 15 min. Spectra were recorded about every 3 min and are shown in the succession of traces that are dotted and dashed in Figure 12. The most intense band at 691 nm occurs after the full 15 min of N_2 purging of the cuvette.

This invention shows that proper combination of core and imide substituents in arene diimides affect molecular and solid-state properties affording materials with unique properties. The results illustrate the relationship between molecular functionality, substituent electronic effects, and air-stability of the corresponding FET devices. The methods of synthesis and separation can be used to improve device performance. This class of arene diimides and/or specific compounds thereof are extremely promising materials for novel applications in electronics, photonics, and opto-electronics.

Pertaining to examples 5-12, ^{1}H NMR spectra were recorded on a Varian 400 MHz NMR spectrometer using TMS as an internal standard. Laser desorption mass spectra were obtained with a Perseptive BioSystems time-of-flight MALDI mass spectrometer using a dithranol matrix. Solvents and reagents were used as received. Flash and thin-layer chromatography was performed using Sorbent Technologies (Atlanta, GA) silica gel. All solvents were spectrophotometric grade. Toluene was purified by CuO and alumina columns (GlassContour).

Optical absorption measurements were made on a Shimadzu (UV-1601) spectrophotometer using 1.0 cm path length cuvettes. Fluorescence quantum yields were obtained by integrating the fluorescence emission bands from each compound and rhodamine 640 using corrected spectra obtained on a PTI photon-counting spectrofluorimeter with 1.0 cm path length cuvettes. The absorbance of each sample was < 0.1 at the excitation wavelength.

Electrochemical measurements were performed using a CH Instruments Model 660A electrochemical workstation. The solvent was tetrahydrofuran containing 0.1 M tetra-*n*-butylammonium hexafluorophosphate electrolyte. A 1.0 mm diameter platinum disk electrode, platinum wire counter electrode, and Ag/Ag_xO reference electrode were employed. The ferrocene/ferrocinium (Fc/Fc^+, 0.52 vs. SCE) was used as an internal reference for all measurements.

Example 5

Synthesis of *N,N'*-bis(1H,1H-perfluorobutyl)-1,7-dibromo-perylene-3,4:9,10-bis(dicarboximide). The reagent 1,7-dibromoperylene-3,4:9,10-

tetracarboxydianhydride was prepared according to the literature. See, Ahrens, et al., *J. Am. Chem. Soc.*, 2004, 126, 8284-8236. The dibromo compound (0.920 g, 1.67 mmol) was combined with 20 mL 1-methyl-2-pyrrolidinone (NMP) and placed in a sonication bath for 20 min. Next, 2,2,3,3,4,4,4-heptafluorobutylamine (Fluorochemicals / SynQuest Labs) in 15 mL NMP was added, followed by addition of acetic acid (0.684 g, mmol). The reaction mixture was heated to 85 - 90° C for 7 h under a N_2 atmosphere. The contents were cooled to room temperature, poured into 200 mL methanol, and placed in a -10° C freezer overnight. The red precipitate was recovered by filtration, dried under a N_2 stream, and chromatographed on silica (chloroform) to afford (1) the bis(perfluoro) compound (1.196 g, 78 %). ^{1}H NMR ($CDCl_3$): δ 9.359 (d, J = 8.15 Hz, 2H), δ 8.822 (s, 2H), δ 8.615 (d, J = 8.15 Hz, 2H), δ 5.009 (m, 4H). M.S.: 912.51 (calcd. 909.88).

Example 6

Synthesis of *N,N'*-bis(1H, 1H-perfluorobutyl)-(1,7 & 1,6)-dicyano-perylene-3,4:9,10-bis(dicarboximide). *N,N'*-bis(1H,1H-perfluorobutyl)-1,7-dibromo-perylene-3,4:9,10-bis(dicarboximide) (1.196 g, 1.31 mmol), zinc cyanide (1.264 g, 10.8 mmol), 1,1'-bis(diphenylphosphino)ferrocene (0.119 g, 0.21 mmol), and tris(dibenzylideneacetone)-dipalladium(0) (0.041 g, 0.04 mmol) were combined in 20 mL p-dioxane and refluxed for 12 h under a N_2 atmosphere. The reaction mixture was then diluted with chloroform, filtered through Celite, and the solvent removed on a rotary evaporator. The resulting crude product was chromatographed on silica using 98% DCM / 2% acetone as the eluent to yield (2) the dicyano compound (0.845 g, 80 %). The product was further purified by high vacuum gradient temperature sublimations. ^{1}H NMR ($CDCl_3$): δ 9.760 (d, J = 6.20 Hz, 2H), δ 9.742 (d, J = 6.22 Hz, 2H), δ 9.100 (s, 2H), δ 9.051 (s, 2H), δ 9.005 (d, J = 8.19 Hz, 2H), δ 8.949 (d, J = 8.17 Hz, 2H), δ 5.048 (m, 4H). M.S.: 804.42 (calcd. 804.05). Anal. Calcd. for $C_{34}H_{10}F_{14}N_4O_4$: C, 50.76, H, 1.25, N, 6.96. Found: C, 50.76, H, 1.34, N, 6.91.

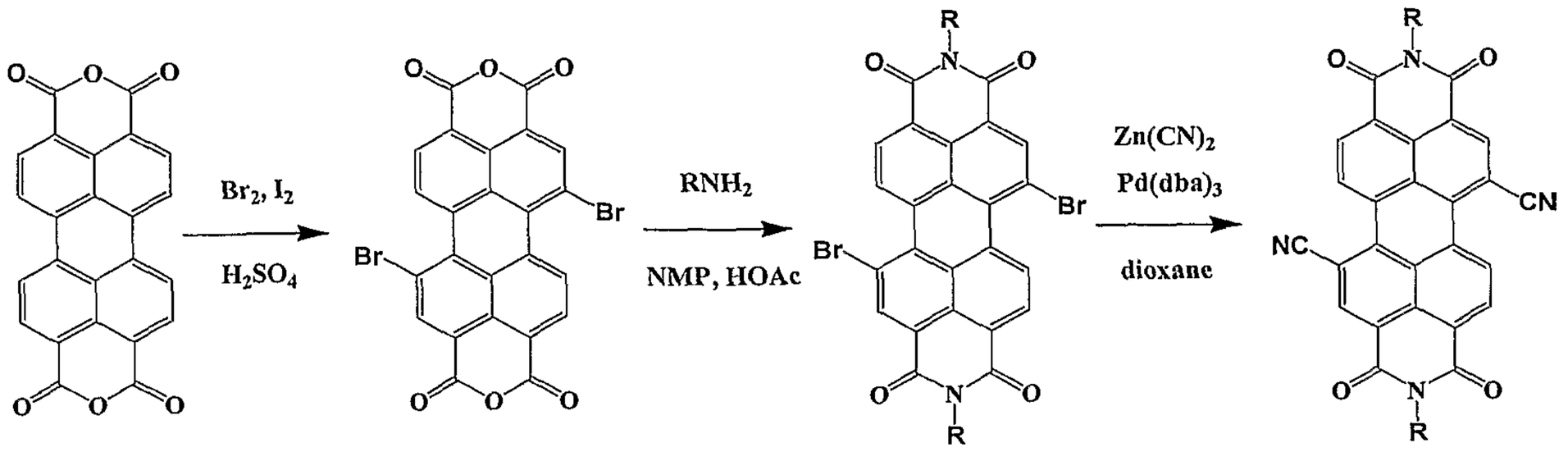

Example 7

Vapor-deposited OFETs in the top-contact configuration were fabricated in the following manner. Films of PDI-FCN_2 and PDI-CN_2 ~ 50 nm thick were vapor deposited (0.2 Å s^{-1}, P ~ 10^{-6} Torr) onto a n^+-doped Si (100) wafer with a 300 nm thermally grown SiO_2 dielectric layer. Gold electrodes 40 nm thick were thermally evaporated onto the thin films through a shadow mask. Silicon substrates were treated with 1,1,1,3,3,3-hexamethyldisilazane vapor prior to film deposition. Substrate temperature during film deposition was varied with a cartridge heater.

Bottom contact devices were fabricated by evaporating 40 nm thick gold electrodes directly onto the HMDS treated silicon substrate followed by deposition of the organic film under the same conditions as above. Alkane thiol treatment of the gold electrodes was accomplished by submerging the substrate in a 10^{-3} M ethanol solution of octadecanethiol for 3 hours. The substrates were then rinsed with ethanol and dried prior to film deposition.

Solution-cast films were fabricated by drip-casting. First, the outer edge of the substrate was coated with Novec-ECC 1700 electronic coating to define an area for solution containment. The substrate was heated to 90 °C, and ~ 1 mL of a 10^{-3} M solution of the material was deposited. During the slow evaporation process, the substrates were protected from atmospheric currents by containment in a glass vessel. Films of PDI-FCN_2 were cast from toluene, while films of PDI-CN_2 were cast from chloroform. A device comprising PDI-FCN_2 was operated in ambient for over 100 cycles with minimal change in device behavior (see, Fig. 14).

Example 8

TGA, SEM, AFM and XRD results for PDI-CN_2 and PDI-FCN_2 films are provided in Figures 15-18, respectively.

Example 9

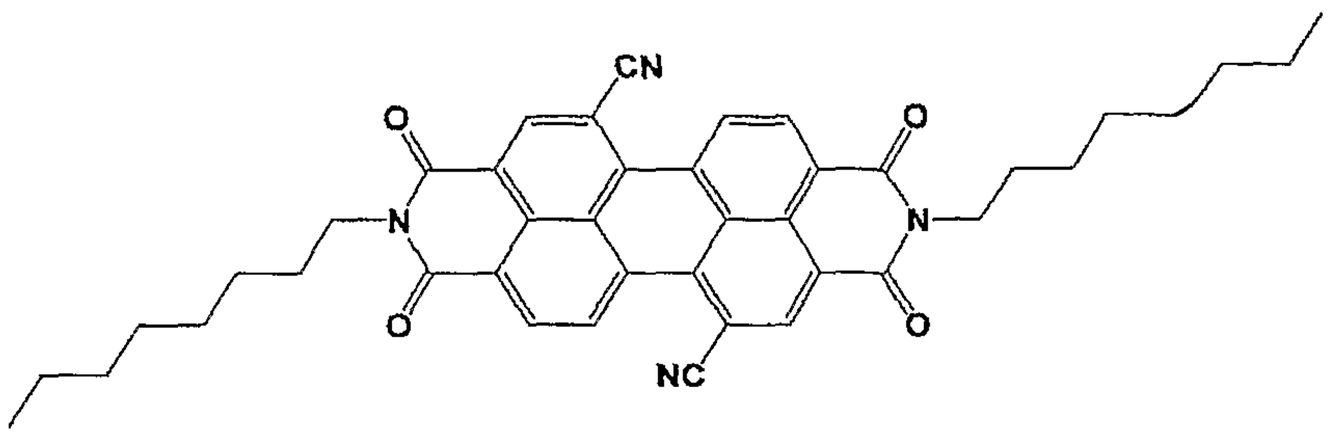

PDI-8CN_2

Synthesis of *N,N'*-bis(n-octyl)-(1,7 & 1,6)-dicyanoperylene-3,4:9,10-bis(dicarboximide), PDI-8CN_2. *N,N'*-bis(n-octyl)-(1,7 & 1,6)-dibromoperylene-3,4:9,10-bis(dicarboximide) (1.318 g, 1.71 mmol) and copper (I) cyanide (1.550 g, 17.31 mmol) were combined in a 50 ml round bottom flask with 20 ml dry DMF. This mixture was placed in a sonication bath for 30 minutes then heated to 130°C under a nitrogen atmosphere for 5 hours. The DMF was then removed under reduced pressure leaving a reddish / brown residue behind. Soxhlet extraction with chloroform for 36 hours provided the title compound as a red powder in 69% yield, (0.777g, 1.17 mmol). Mass spectrum (m/z) 663.10 (calc. 664.30) ^{1}H NMR ($CDCl_3$) Integrations reported are for the 1,7 isomer (~90% pure) ([ ] indicates 1,6 or 1,7isomer): δ 9.700 (d, J = 8.2 Hz, [1,7 (1,6 unresolvable)] 2H), 9.023 (s, [1,6]), 8.972 (s, [1,7], 2H), 8.924 (d, J = 8.2 Hz, [1,7], 2H), 8.863 (d, J = 8.2 Hz, [1,6]), 4.219 (m, 4H), 1.763 (m, 4H), 1.45 — 1.20 (m, 20H), 0.884 (t, J = 6.7 Hz, 6H). (The dicarboximide was prepared according to Ulrike, et al., *J. Mat. Chem.* (2001), 11(7), 1789-1799.)

Example 10

The electronic properties of PDI-8CN_2 (N-octyl) are virtually indistinguishable from that of PDI-CN_2 (N-cyclohexy), with an absorption maximum at 530 nm, emission maximum at 547 nm, and first reduction potential of -0.1 vs. S.C.E. placing the HOMO at ~6.6 eV and the LUMO at

~4.3 eV vs. vacuum level. The reduced pressure (5 Torr) TGA of PDI-8CN_2 reveals that the material evaporates with less than 10% decomposition at ~325°C. Simultaneously acquired DTA data reveals a solid-liquid transition prior to evaporation at ~300 °C.

Example 11

Films of PDI-8CN_2 were deposited from the vapor phase onto analogous substrates as used in the studies on PDI-CN_2 and PDI-FCN_2. Gold electrodes in the top-contact configuration were also deposited in the same manner as before.

Example 12

Transistors were characterized as before. At substrate temperatures during deposition of >90 °C, mobilities as high as 0.2 $cm^2 V^{-1} s^{-1}$ are observed. The devices have threshold voltages of ~ -6 V and I_{ON}/I_{OFF} ratios as high as 10^4. (See Figure 19.) These devices also operate under both inert and ambient atmosphere with negligible differences.

Example 13

With reference to Table 3, below, this example further illustrates perylene compounds, materials and/or films of the type available through this invention. Such compounds can comprise any moiety R^9 and/or R^{10} combination with at least one of the substituents and moieties for any one or more of R^1-R^{10}, R^{11}, and R^{12}. Such N- and core-substituted compounds are available through the synthetic techniques described herein or straight forward modifications thereof as would be understood by those skilled in the art. With reference to example 6, preparation of a desired imide is limited only by choice of amine reagent and the corresponding mono- or dianhydride starting material. For instance, R^9 and/or R^{10} can be an alkyl (substituted or insubstituted) or polyether moiety through use of the respective amino-terminated alkyl reagent or ethylene glycol oligomer. Likewise, various core substituents can be introduced by chemistry on commercially-available perylene anhydrides or bromo-substituted analogs thereof, using variations of aromatic acylation, alkylation and/or substitution reactions known in the art (e.g., Cu-catalyzed

fluoroalkyl substitution reactions described in U.S. Patent No. 6,585,914, the entirety of which may be referred to for further details. In an analogous manner, a comparable range of N- and core-substituted naphthalene compounds are available from the corresponding starting materials and reagents.

Table 3

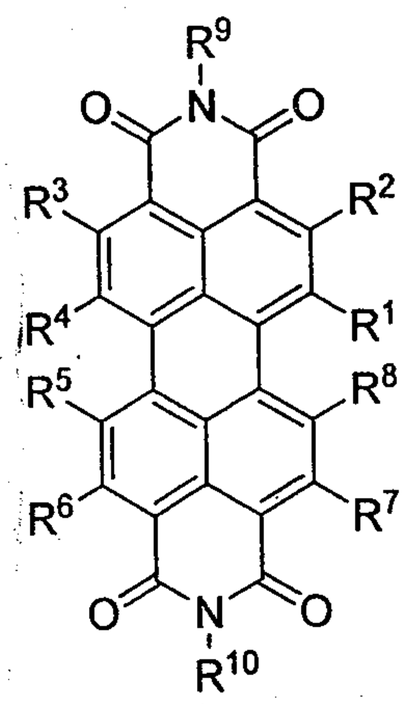

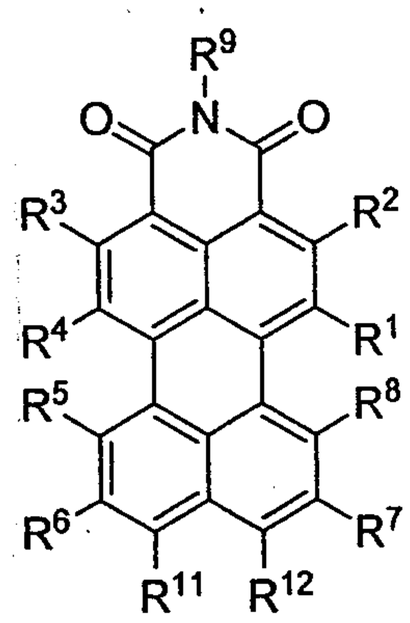

R^9	R^1-R^8, R^{11}, and R^{12}
H, $(CH_2)_2CF_3$, C_5HF_8, C_6F_5, $C_8H_2F_{15}$, C_6H_4X; (X=H, Cl, F, $^+N(CH_3)_3$), $C_{16}H_{31}F_3$, any of R^{10}	H, CN, NO_2, halide, SO_3H, $^+N(R)_3$; (R=H, alkyl), CH_2CF_3, C(O)R; (R=H, alkyl, phenyl), CO_2R; (R=H, alkyl, phenyl), C_6H_4X; (X=H, F, CN, NO_2)

R^{10}
Any of R^9, $C_6H_9F_2$ C_5H_{12}, $C_8H_{14}F_3$, C_6H_4X; X=H, CN, NO_2 $(CH_2CH_2O)_nC_2H_4OH$; n = 1 - 7

WHAT IS CLAIMED IS:

1. A compound of a formula selected from

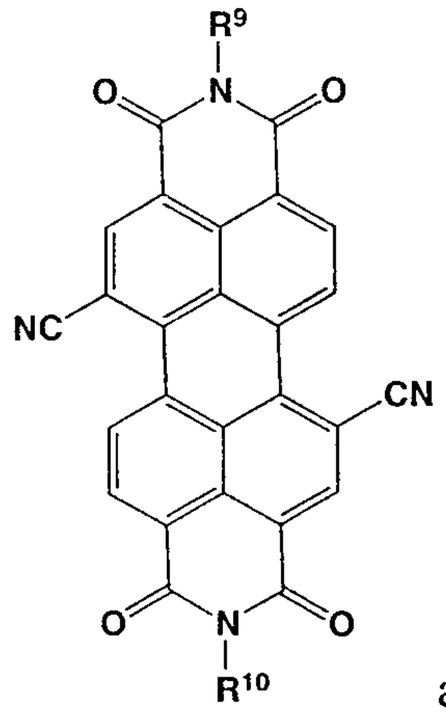

and

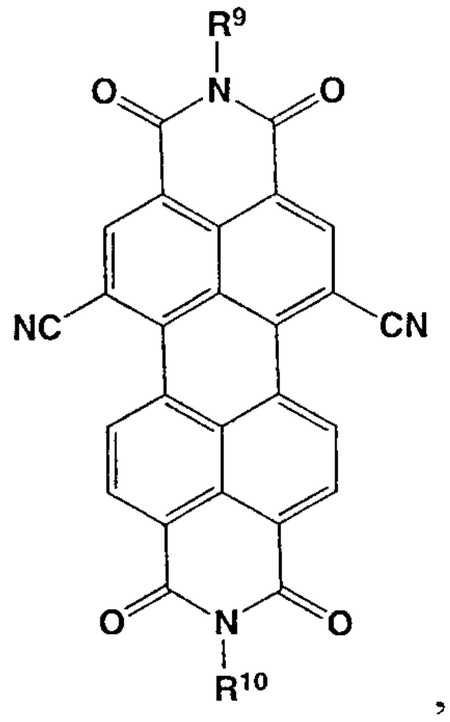

,

wherein R^9 and R^{10} are selected from C_n alkyl moieties and halo-substituted C_n alkyl moieties, wherein n ranges from 3 to 16.

2. The compound of claim 1, wherein R^9 and R^{10} are C_nH_{2n+1}, and n ranges from 3 to 16.

3. The compound of claim 1, wherein R^9 and R^{10} are fluoro-substituted C_n alkyl moieties, wherein n ranges from 3 to 16.

4. The compound of claim 1, wherein R^9 and R^{10} are C_nF_{2n+1}, and n ranges from 3 to 16.

5. The compound of claim 1, wherein R^9 and R^{10} are $C_nH_2F_{2n-1}$, and n ranges from 3 to 16.

6. A composite comprising a substrate and a semiconductor component thereon, said semiconductor component comprising a compound of a formula selected from

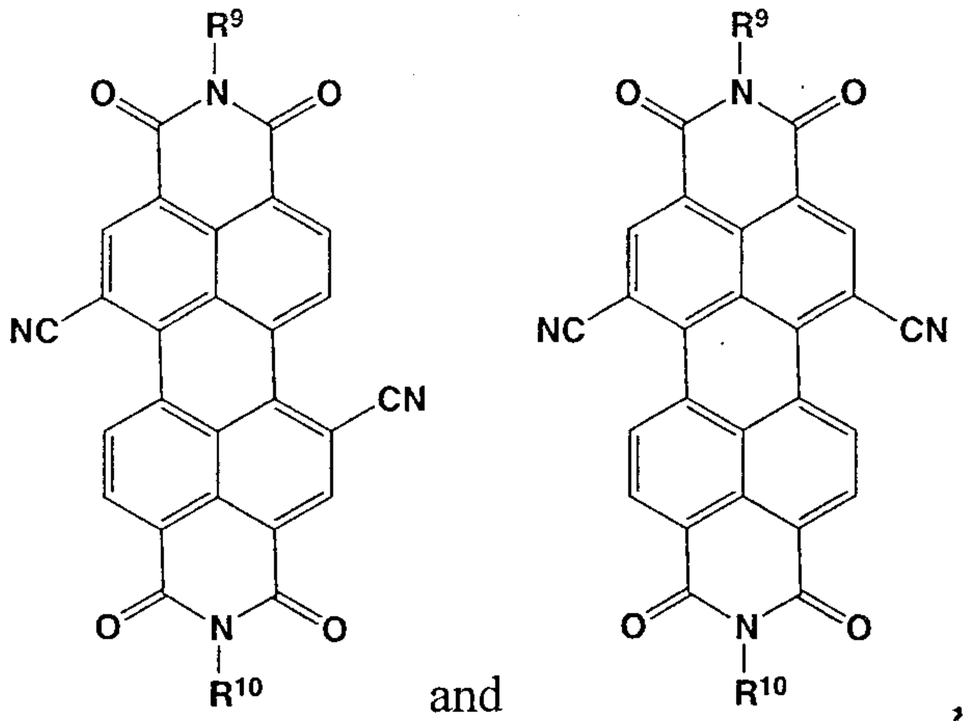

and

,

wherein R^9 and R^{10} are selected from C_n alkyl moieties and halo-substituted C_n alkyl moieties, wherein n ranges from 3 to 16.

7. The composite of claim 6, wherein R^9 and R^{10} are C_nH_{2n+1}, and n ranges from 3 to 16.

8. The composite of claim 6, wherein R^9 and R^{10} are fluoro-substituted C_n alkyl moieties, wherein n ranges from 3 to 16.

9. The composite of claim 6, wherein R^9 and R^{10} are C_nF_{2n+1}, and n ranges from 3 to 16.

10. The composite of claim 6, wherein R^9 and R^{10} are $C_nH_2F_{2n-1}$, and n ranges from 3 to 16.

11. An organic field effect transistor (OFET) device comprising the composite of claim 6.

12. The OFET device of claim 11, wherein the semiconductor component is vapor-deposited onto the substrate.

13. The OFET device of claim 12, wherein the OFET device has a top-contact configuration.

14. The OFET device of claim 12, wherein the OFET device has a bottom-contact configuration.

15. The OFET device of claim 11, wherein the semiconductor component is solution-cast onto the substrate.

16. The OFET device of claim 15, wherein the OFET device has a top-contact configuration.

17. The OFET device of claim 15, wherein the OFET device has a bottom-contact configuration.

18. An organic field effect transistor (OFET) device comprising the composite of claim 7.

19. The OFET device of claim 18, wherein the semiconductor component is vapor-deposited onto the substrate.

20. The OFET device of claim 19, wherein the OFET device has a top-contact configuration.

21. The OFET device of claim 19, wherein the OFET device has a bottom-contact configuration.

22. The OFET device of claim 18, wherein the semiconductor component is solution-cast onto the substrate.

23. The OFET device of claim 22, wherein the OFET device has a top-contact configuration.

24. The OFET device of claim 22, wherein the OFET device has a bottom-contact configuration.

25. An organic field effect transistor (OFET) device comprising the composite of claim 8.

26. The OFET device of claim 25, wherein the semiconductor component is vapor-deposited onto the substrate.

27. The OFET device of claim 26, wherein the OFET device has a top-contact configuration.

28. The OFET device of claim 26, wherein the OFET device has a bottom-contact configuration.

29. The OFET device of claim 25, wherein the semiconductor component is solution-cast onto the substrate.

30. The OFET device of claim 29, wherein the OFET device has a top-contact configuration.

31. The OFET device of claim 29, wherein the OFET device has a bottom-contact configuration.

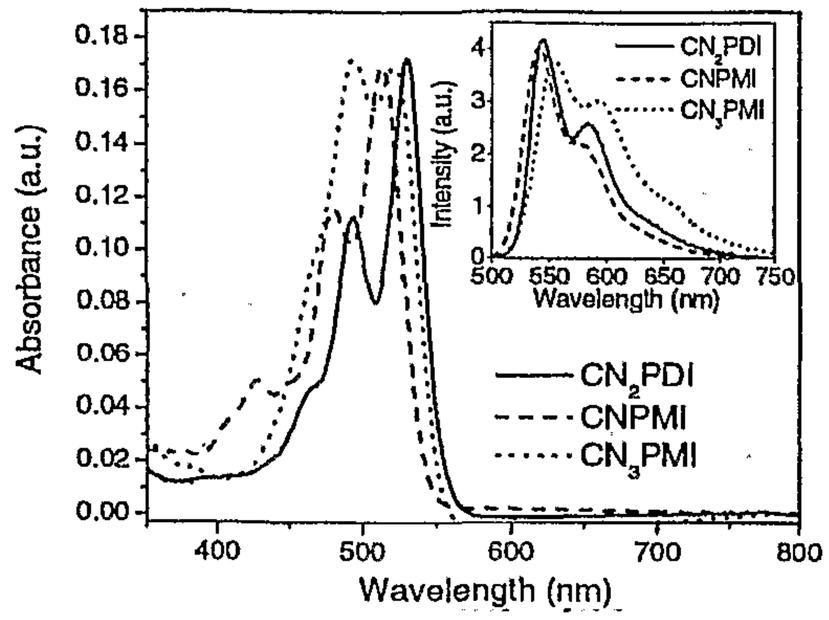

Figure 1

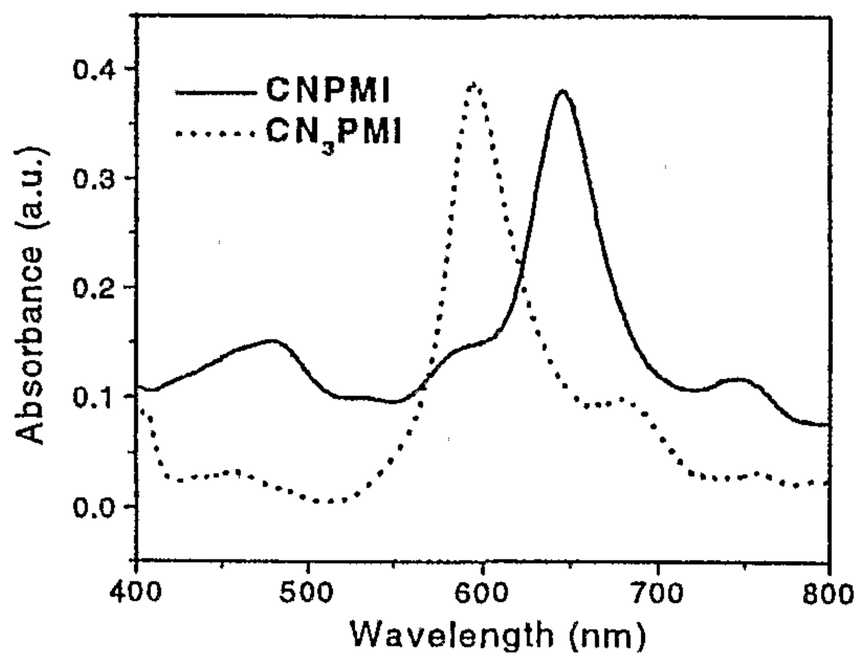

Figure 2

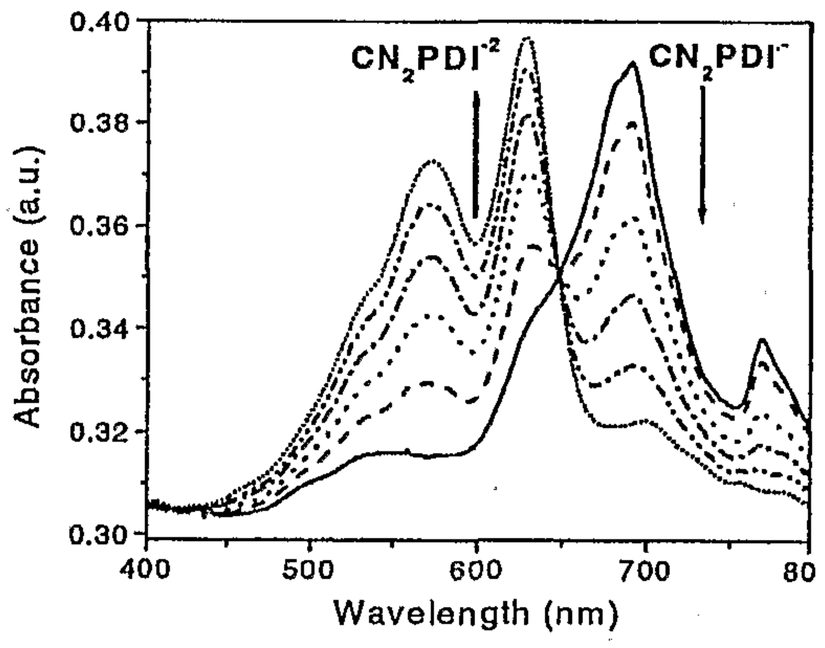

Figure 3

Figure 4

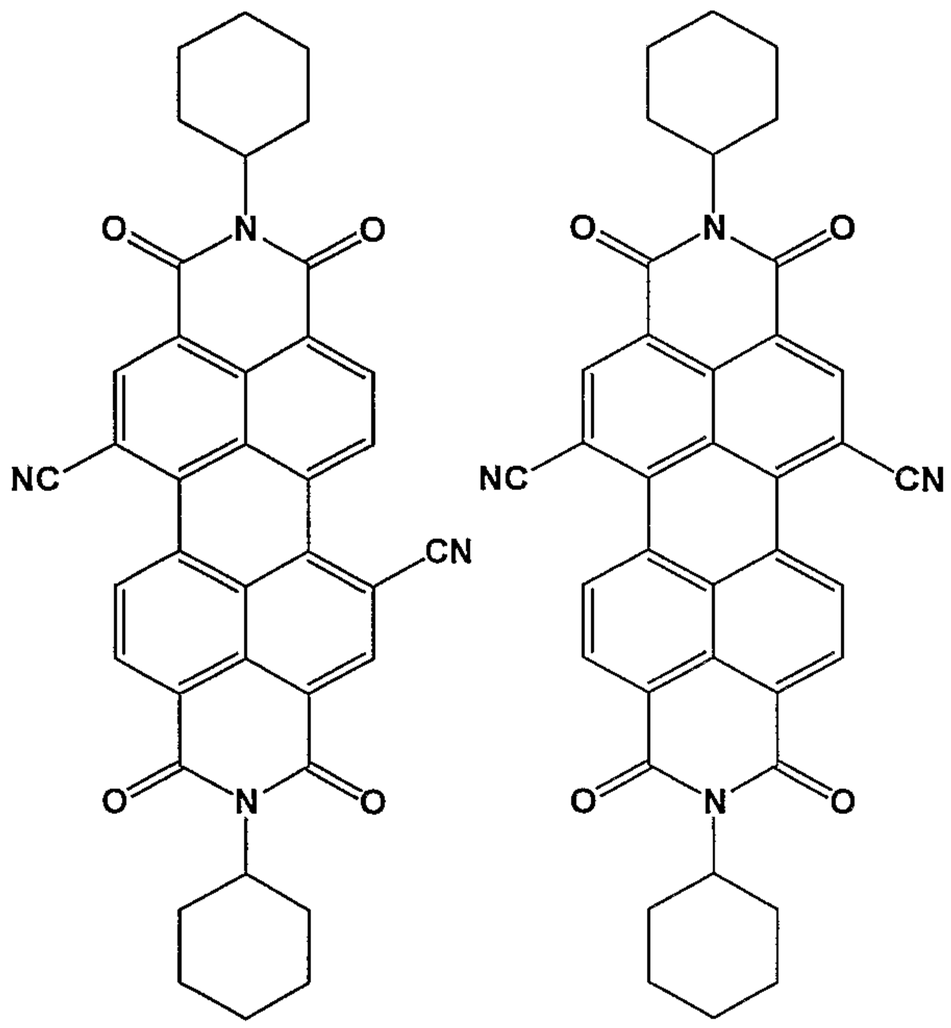

tCN_2PDI *c*CN_2PDI

Figure 5

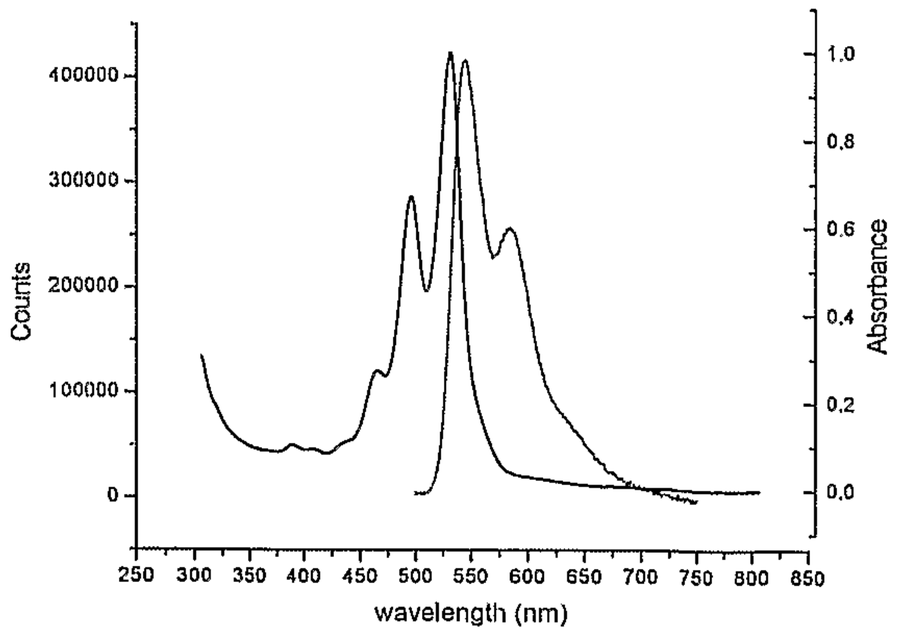

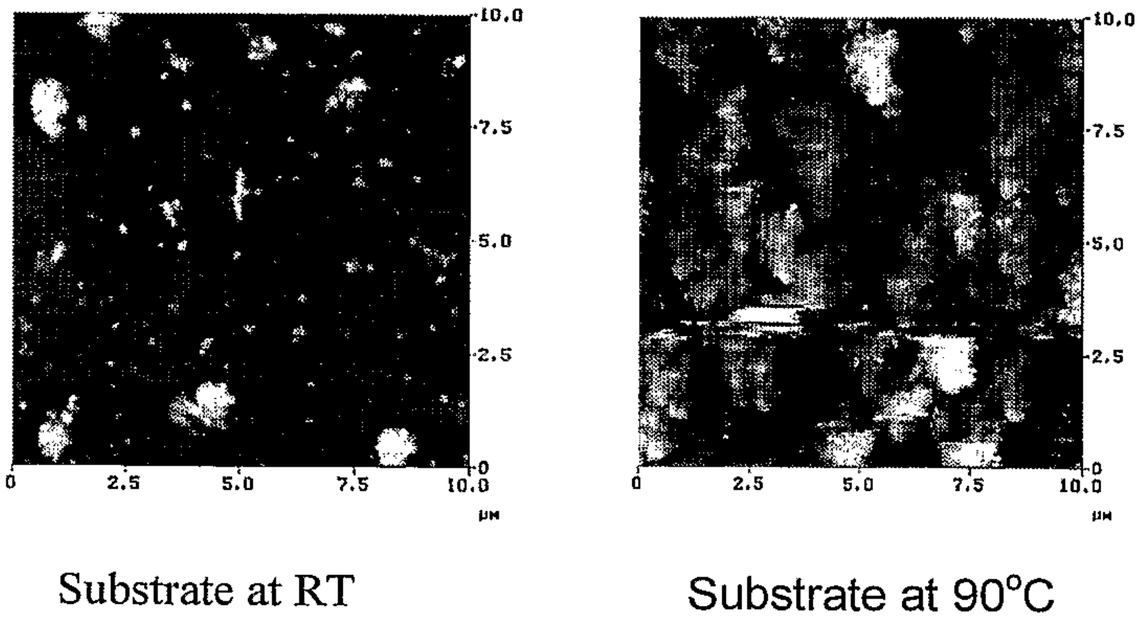

Substrate at RT Substrate at 90°C

Figure 6

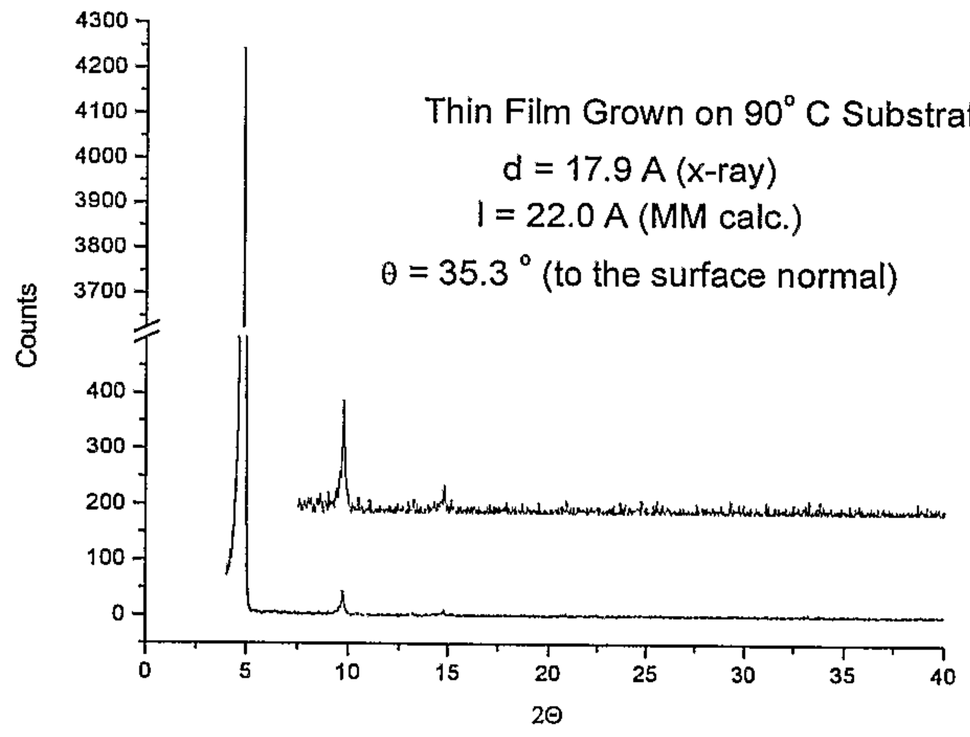

Figure 7

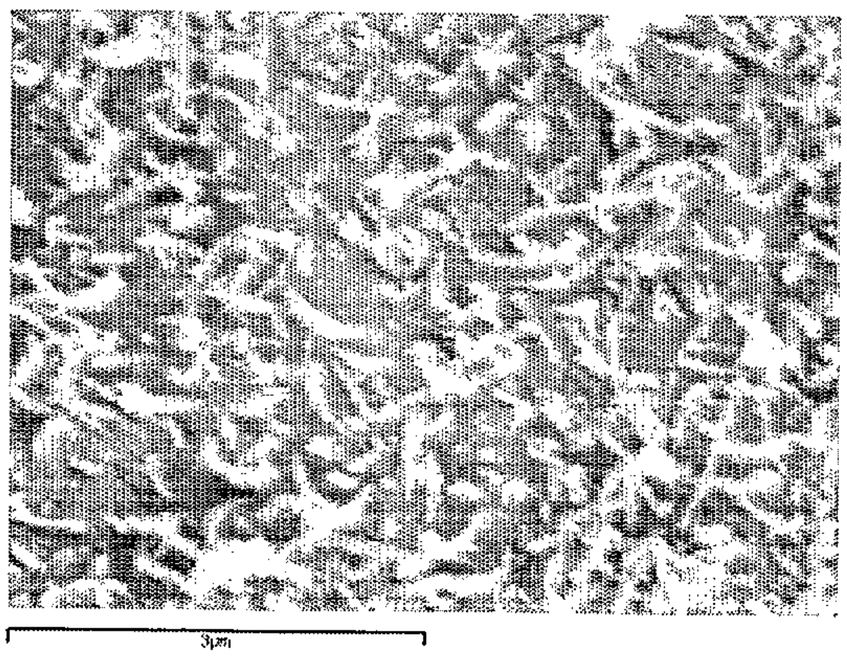

Figure 8

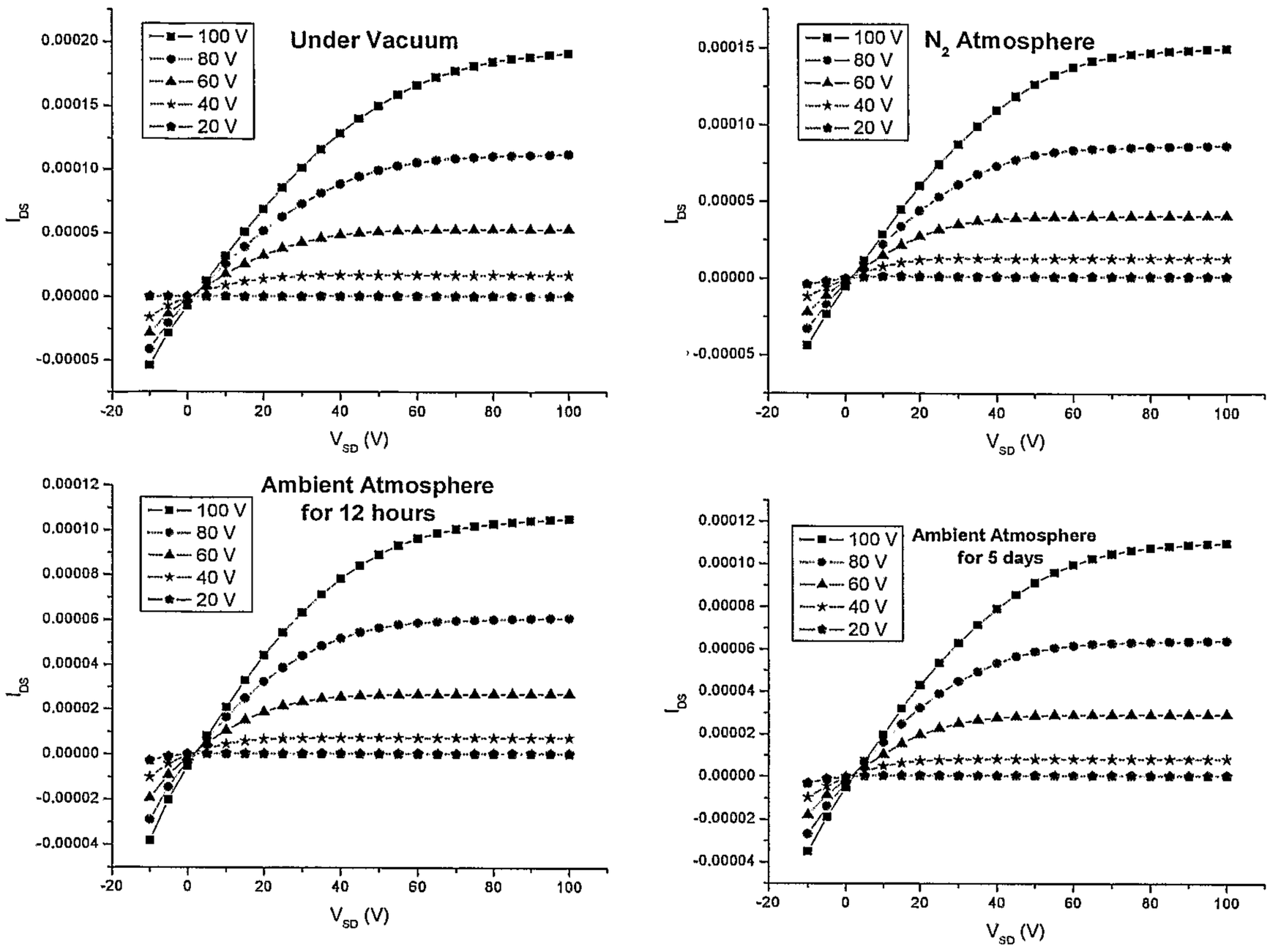

Figure 9

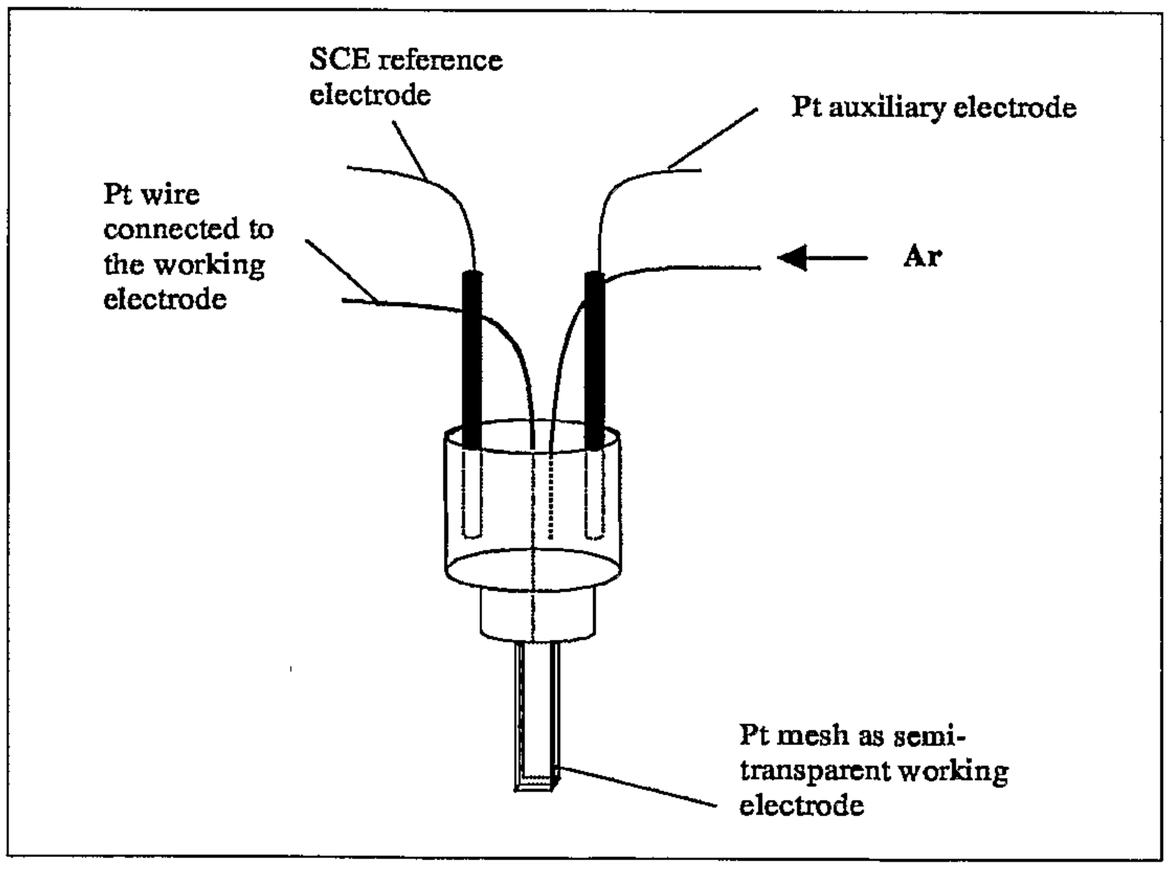

Figure 10

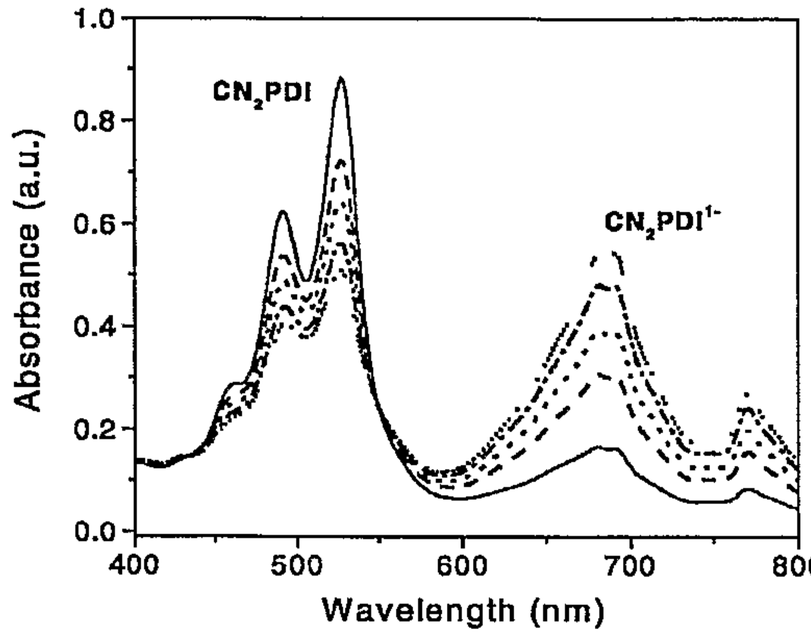

Figure 11

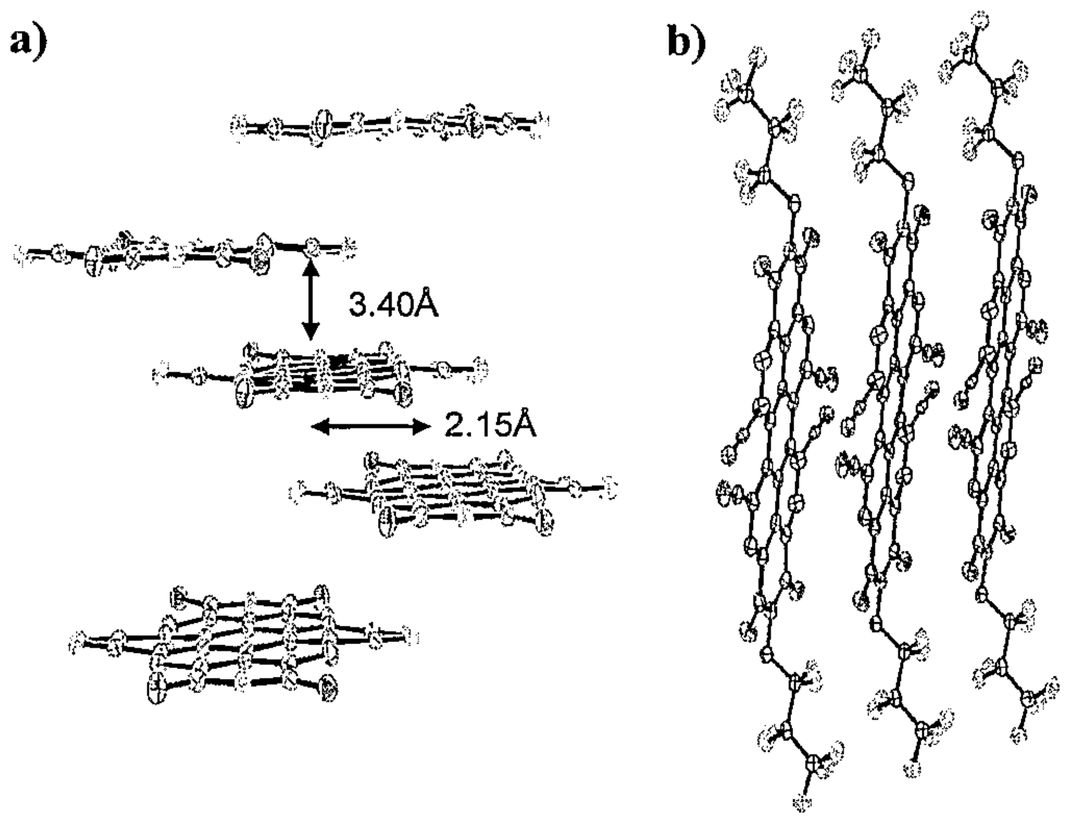

Figure 12

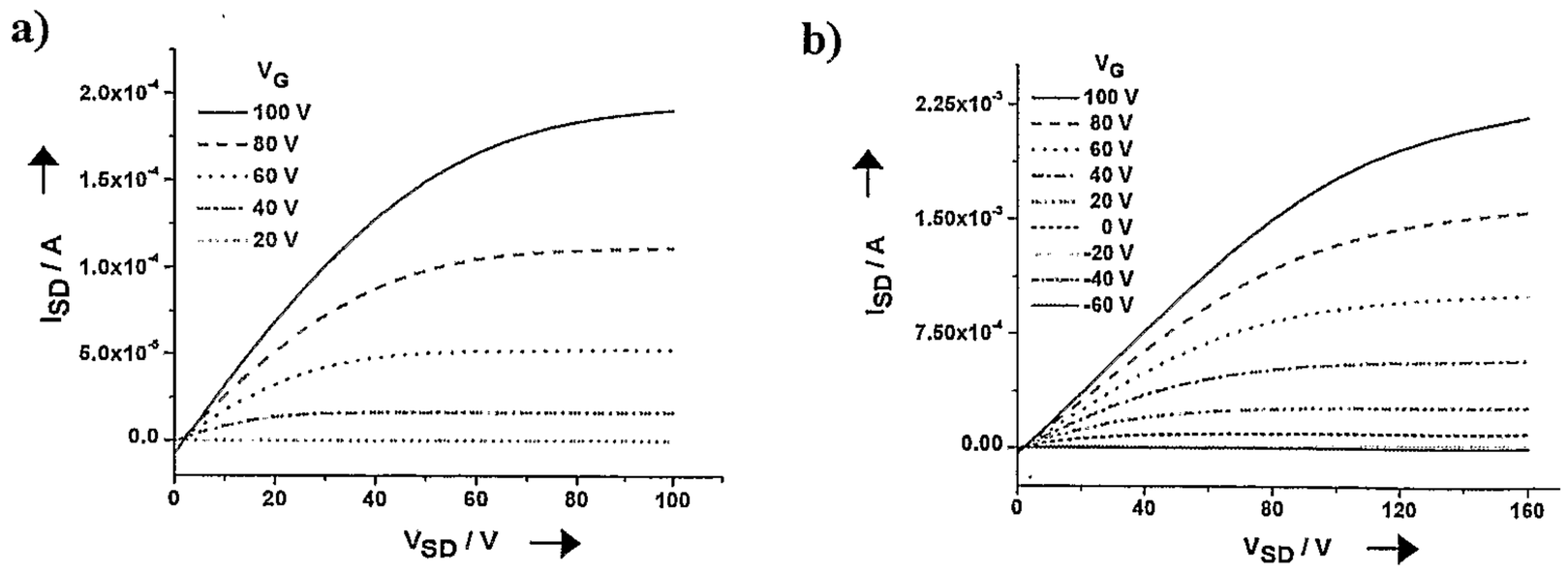

Figure 13

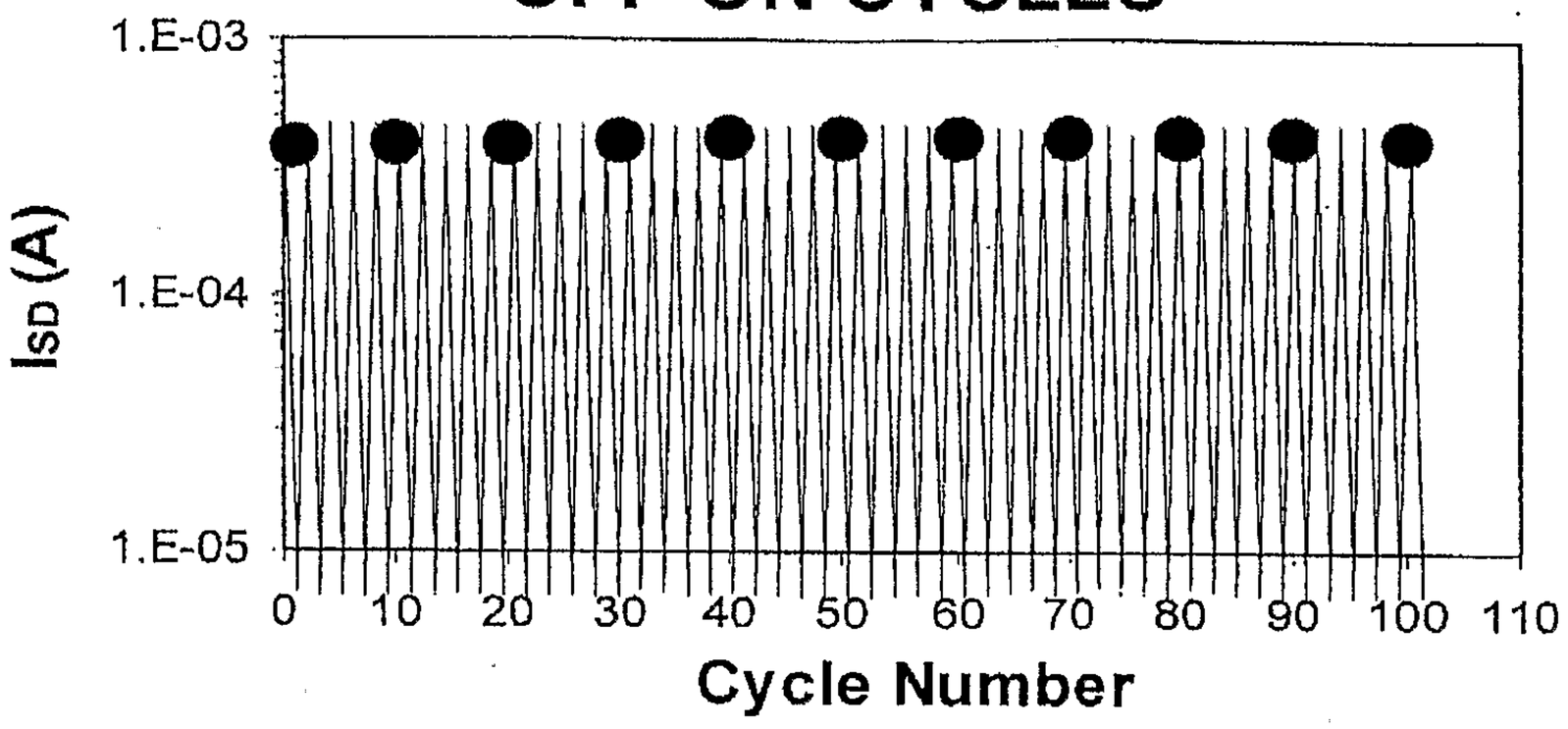

Figure 14

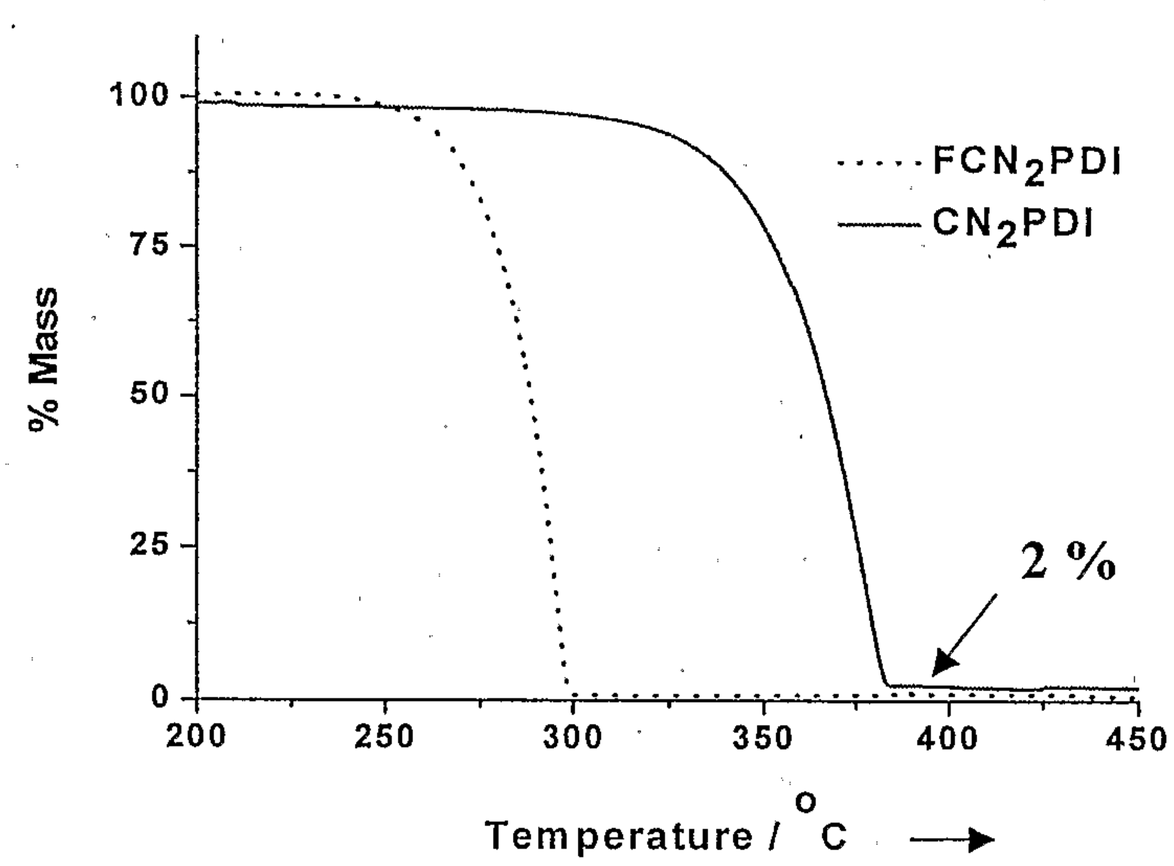

Figure 15

a)

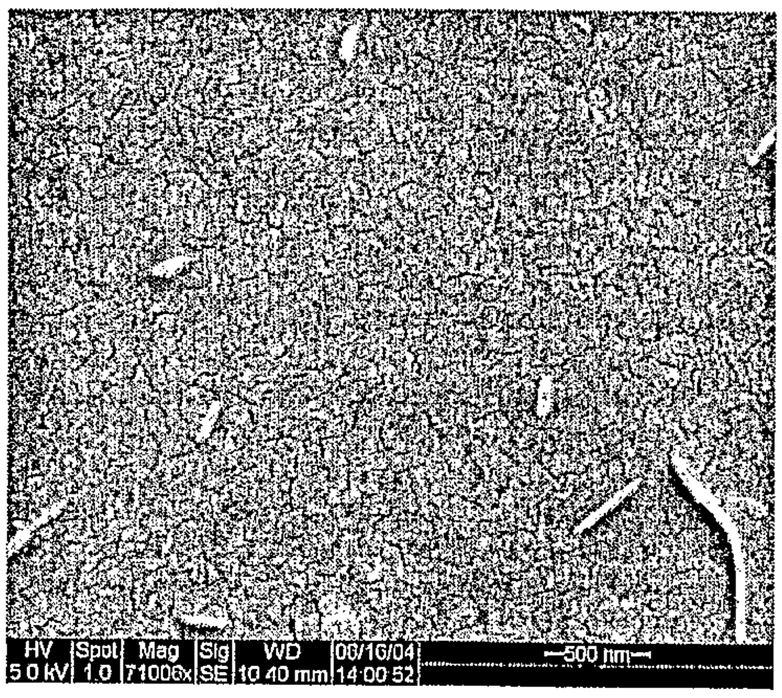

b)

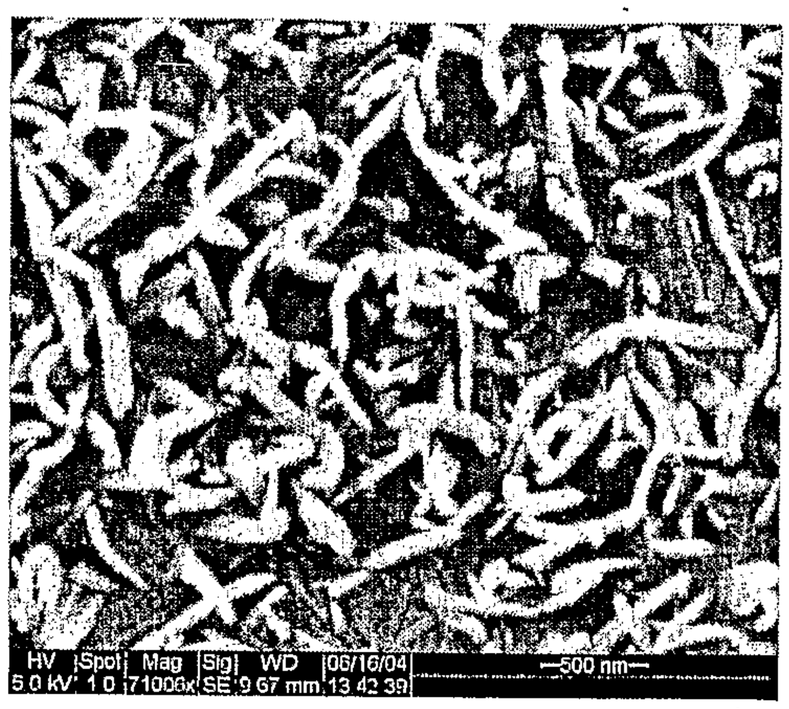

Figure 16

a)

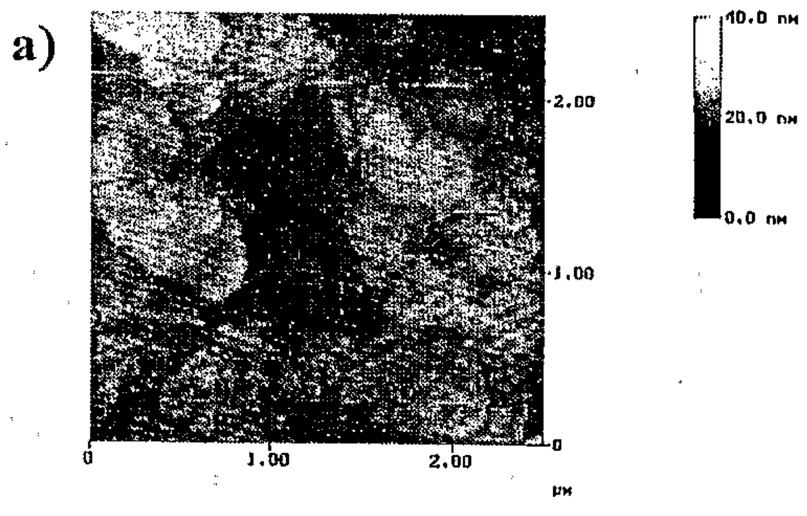

b)

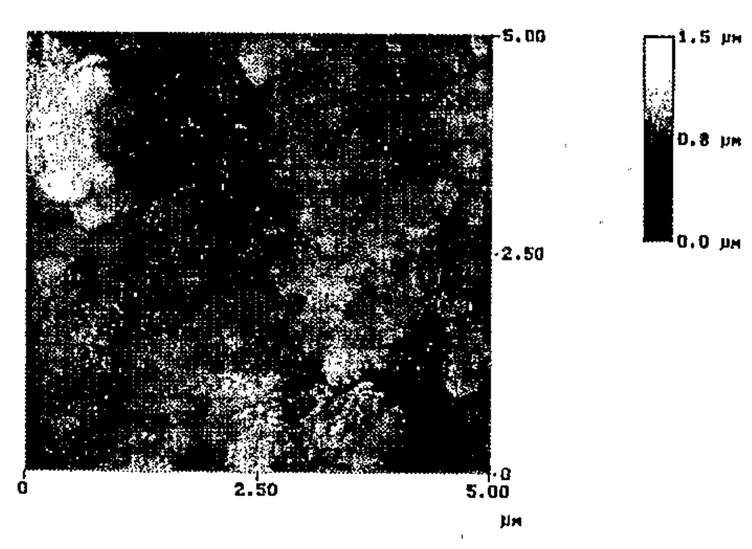

Figure 17

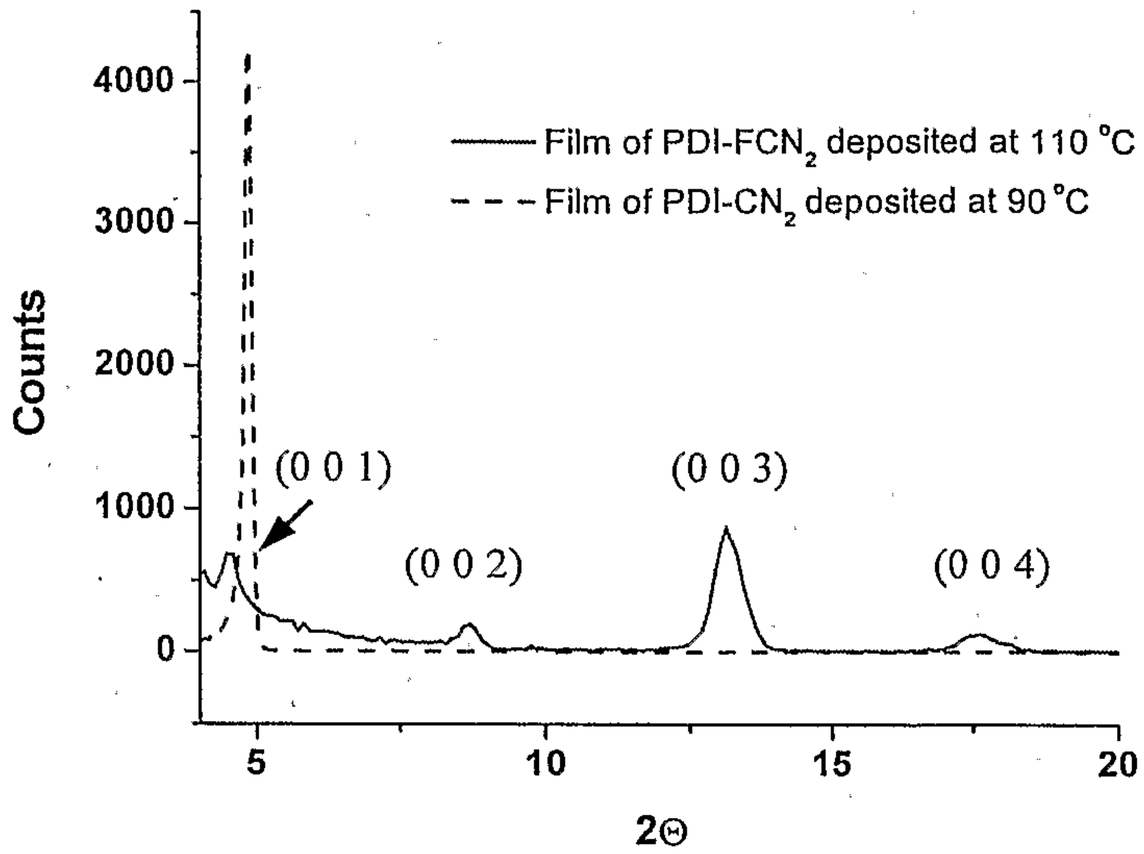

Figure 18

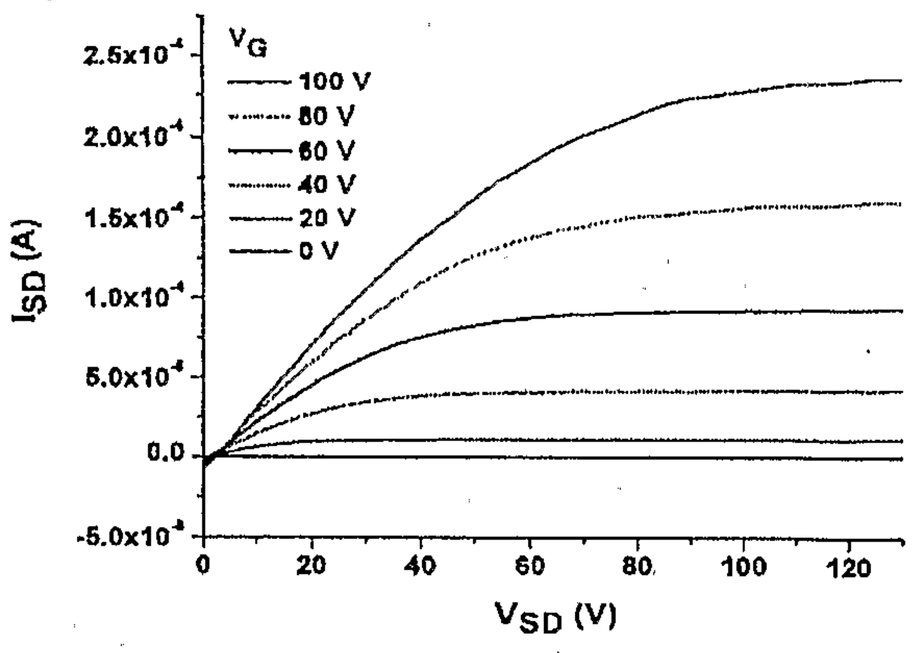

Figure 19

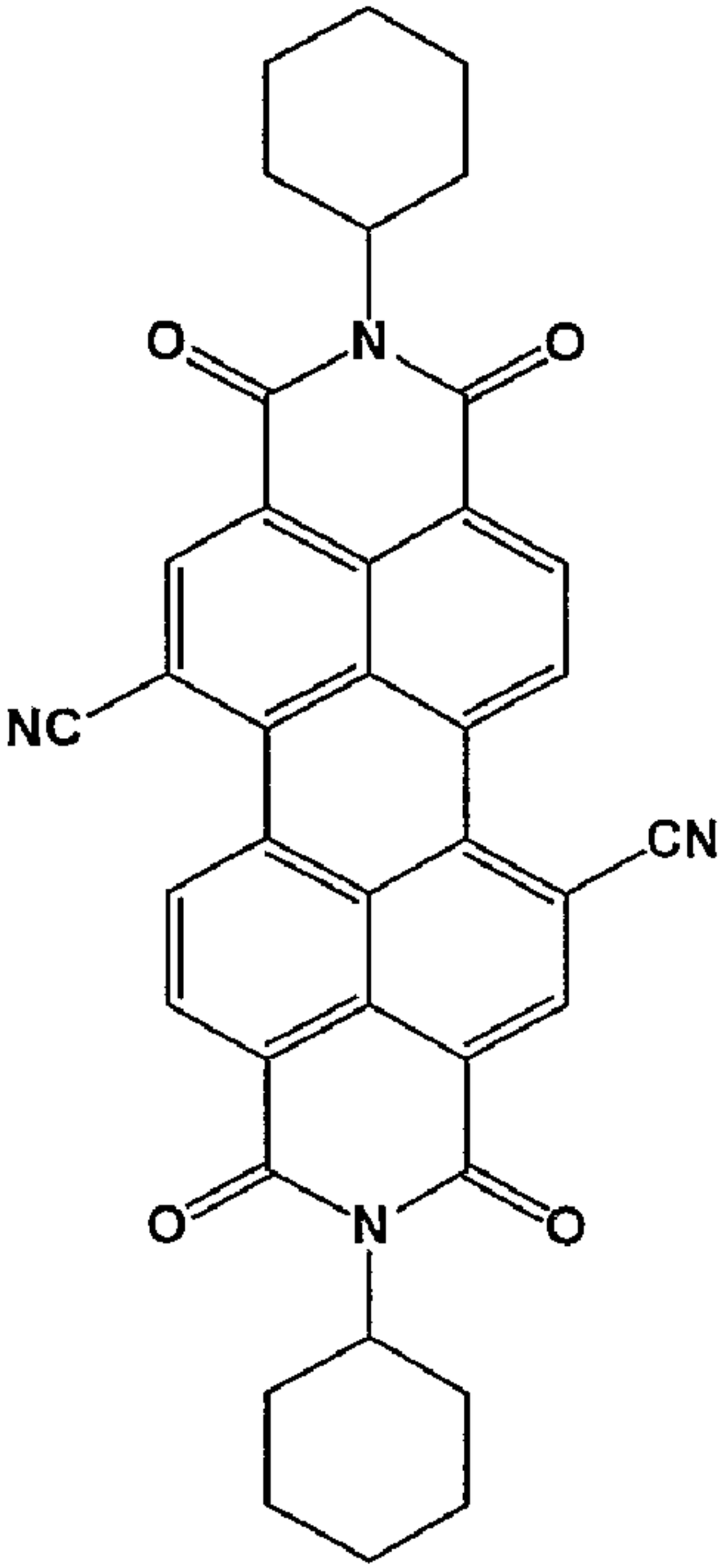

tCN_2PDI

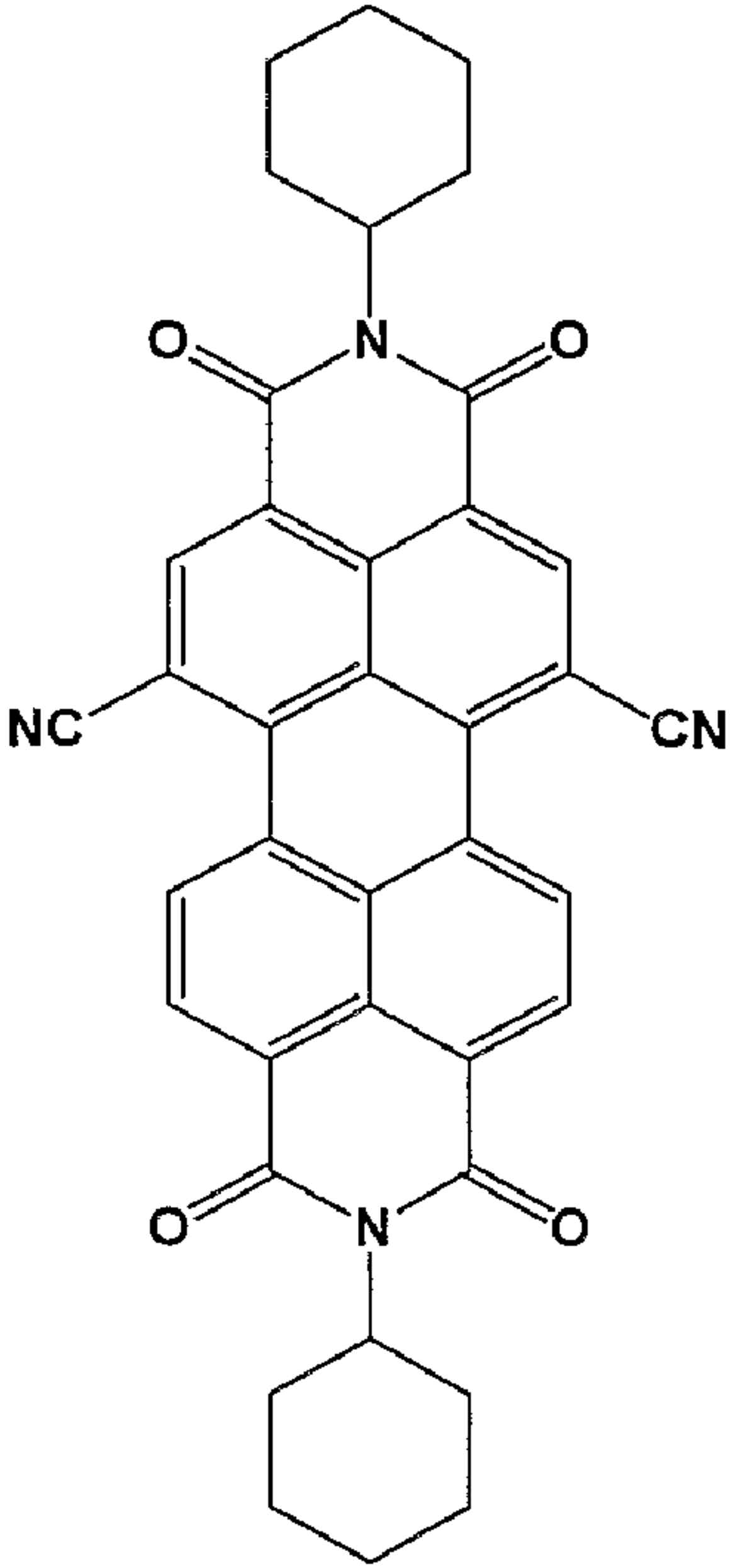

cCN_2PDI